chromosome array-based methylated CpG island amplification (BAMCA) studies indicate significant differences in the methylation patterns present in HBV- and HCV-associated HCC [59]. The HBx protein expressed by HBV may influence cellular methyltransferase activity, and could possibly contribute to altered methylation patterns [60]. An additional possibility is that epigenetic differences in HBV- and HCV-associated HCC could reflect different cell types from which the cancer originates, as HBV may be capable of infecting hepatocyte progenitors [61].

Our results also show that miR-122 expression is reduced in non-tumor liver tissue from HCV-infected persons. In contrast, contrary to a recent report by Wang et al. [54], we found that miR-122 is expressed at normal levels in non-tumor HBV-infected liver (Figure 2). Several lines of evidence suggest that this difference may reflect a more active IFN response in HCV- versus HBV- infected livers. In vitro studies suggest that IFN-β inhibits miR-122 expression [36,62], and HCV stimulates a more robust intrahepatic innate immune response than HBV [63,64]. Consistent with this, our results reveal a correlation between miR-122 abundance in non-tumor tissues and IL28B genotype, defined by a single nucleotide polymorphism (rs8099917) associated with response to Peg-IFN/RBV as well as endogenous pre-treatment ISG expression levels (Figure 5A) [40,41]. We also found an inverse relationship between the abundance of several ISG transcripts and miR-122 (Figure 5C). Interestingly, this relationship was not observed in tumor tissues from these patients, suggesting that genetic or epigenetic changes alter miR-122 regulation in HCC tissue, or that the cancer cells are refractory to stimulation by type 1 IFNs.

Consistent with our findings in HCV-infected patients, we also observed a reduction in miR-122 abundance in liver tissue from HCV-infected chimpanzees (Figure 4A), and an inverse correlation between the abundance of HCV RNA in the liver and serum HCV RNA levels (Figure 4B). Although Sarasin-Filopowicz et al. [36] demonstrated a trend toward lower miR-122 abundance in liver tissues with high viral RNA copy numbers, this did not achieve statistical significance and no correlation was evident between serum RNA levels and miR-122 abundance in the patients studied by this group. It is not clear why such a relationship exists in chimpanzees but not infected humans. One possibility is that it might be related to the fact that chimpanzees generally have very robust intrahepatic innate immune responses to HCV, with uniformly high levels of intrahepatic ISG expression [65]. The uniformly high intrahepatic innate immune response in chimpanzees contrasts with extensive variation in the intensity of ISG responses in HCV-infected humans [39], possibly allowing for a negative correlation between serum viral RNA level and miR-122 abundance to become manifest.

Finally, our results indicate that miR-191 expression may be increased in HBV-associated HCC (Figure 6). This supports a previous study in which miR-191 abundance was increased in HCC of mixed origin, but predominantly associated with HBV infection [42]. miR-191 antagonism has been shown to have anti-tumor potential in studies of Hep3B and SNU423 cells [42], which are both derived from HBV-associated cancers. Our data suggest that elevations of miR-191 are confined to HBV-associated liver cancer (Figure 6), and suggest that virus-specific differences in miRNA signatures may be important in understanding the origins of liver cancer. While these differences may be predictive of response to specific therapeutic interventions, they are unlikely to be of sufficient magnitude or specificity to guide therapy in individual patients.

Supporting Information

Figure S1. U6 snRNA copy number as a standard for normalization of miR-122 abundance. (**A**) U6 copy number (relative copy number per μg RNA) plotted as a function of the RNA integrity number (RIN score, on a scale of 1 to 10) determined as described in Methods in the main text. A strong negative correlation exists between U6 copy number and the RIN score: Spearman r_s = 0.5216, two-tailed p = 0.0001). (**B**) miR-122 abundance in HCC and non-tumor tissues from HBV- and HCV-infected subjects, normalized to U6 snRNA copy number. Statistical significance was assessed using paired and unpaired t tests, as described in the main text.
(TIF)

Author Contributions

Conceived and designed the experiments: CS MH SRS REL SML. Performed the experiments: CS SRS DY TS. Analyzed the data: CS MH SRS DY REL SML. Contributed reagents/ materials/analysis tools: MH SK REL. Wrote the manuscript: CS SML.

References

1. Ferlay JSH, Bray F, Forman D, Mathers C, Parkin DM (2010). ancer Incidence Mortal Worldwide IARC CancerBase No. 10
2. Wang XGJ, Thorgeirsson S, editors (2011) Molecular Genetics of Liver Neoplasia. New York: Springer Verlag Science. pp. 51-73.
3. Lok AS, Everhart JE, Wright EC, Di Bisceglie AM, Kim HY et al. (2011) Maintenance peginterferon therapy and other factors associated with hepatocellular carcinoma in patients with advanced hepatitis C. Gastroenterology 140: 840-849. doi:10.1053/j.gastro.2010.11.050. PubMed: 21129375.
4. White D, El-Serag H (2011) Epidemiology of Hepatocellular Carcinoma. In: X Wang[!(surname)!]S Thorgeirsson. Molecular Genetics of Liver Neoplasia. New York, NY: Springer Verlag Science. pp. 51-73.
5. Kiyosawa K, Umemura T, Ichijo T, Matsumoto A, Yoshizawa K et al. (2004) Hepatocellular carcinoma: recent trends in Japan. Gastroenterology 127: S17-S26. doi:10.1053/j.gastro.2004.03.068. PubMed: 15508082.
6. McGivern DR, Lemon SM (2011) Virus-specific mechanisms of carcinogenesis in hepatitis C virus associated liver cancer. Oncogene 30: 1969-1983. doi:10.1038/onc.2010.594. PubMed: 21258404.
7. Tsai WL, Chung RT (2010) Viral hepatocarcinogenesis. Oncogene 29: 2309-2324. doi:10.1038/onc.2010.36. PubMed: 20228847.
8. Nakamoto Y, Guidotti LG, Kuhlen CV, Fowler P, Chisari FV (1998) Immune pathogenesis of hepatocellular carcinoma. J Exp Med 188: 341-350. doi:10.1084/jem.188.2.341. PubMed: 9670046.
9. Lerat H, Honda M, Beard MR, Loesch K, Sun J et al. (2002) Steatosis and liver cancer in transgenic mice expressing the structural and nonstructural proteins of hepatitis C virus. Gastroenterology 122: 352-365. doi:10.1053/gast.2002.31001. PubMed: 11832450.

10. McGivern DR, Lemon SM (2009) Tumor suppressors, chromosomal instability, and hepatitis C virus-associated liver cancer. Annu Rev Pathol 4: 399-415. doi:10.1146/annurev.pathol.4.110807.092202. PubMed: 18928409.
11. Wilson RC, Doudna JA (2013) Molecular mechanisms of RNA interference. Annu Rev Biophys 42: 217-239. doi:10.1146/annurev-biophys-083012-130404. PubMed: 23654304.
12. Djuranovic S, Nahvi A, Green R (2011) A parsimonious model for gene regulation by miRNAs. Science 331: 550-553. doi:10.1126/science.1191138. PubMed: 21292970.
13. Meijer HA, Kong YW, Lu WT, Wilczynska A, Spriggs RV et al. (2013) Translational repression and eIF4A2 activity are critical for microRNA-mediated gene regulation. Science 340: 82-85. doi:10.1126/science.1231197. PubMed: 23559250.
14. Chang J, Nicolas E, Marks D, Sander C, Lerro A et al. (2004) miR-122, a mammalian liver-specific microRNA, is processed from hcr mRNA and may downregulate the high affinity cationic amino acid transporter CAT-1. RNA Biol 1: 106-113. doi:10.4161/rna.1.2.1066. PubMed: 17179747.
15. Lanford RE, Hildebrandt-Eriksen ES, Petri A, Persson R, Lindow M et al. (2010) Therapeutic silencing of microRNA-122 in primates with chronic hepatitis C virus infection. Science 327: 198-201. doi:10.1126/science.1178178. PubMed: 19965718.
16. Bai S, Nasser MW, Wang B, Hsu SH, Datta J et al. (2009) MicroRNA-122 inhibits tumorigenic properties of hepatocellular carcinoma cells and sensitizes these cells to sorafenib. J Biol Chem 284: 32015-32027. doi:10.1074/jbc.M109.016774. PubMed: 19726678.
17. Lewis AP, Jopling CL (2010) Regulation and biological function of the liver-specific miR-122. Biochem Soc Trans 38: 1553-1557. doi:10.1042/BST0381553. PubMed: 21118125.
18. Jopling CL, Yi M, Lancaster AM, Lemon SM, Sarnow P (2005) Modulation of hepatitis C virus RNA abundance by a liver-specific MicroRNA. Science 309: 1577-1581. doi:10.1126/science.1113329. PubMed: 16141076.
19. Shimakami T, Yamane D, Jangra RK, Kempf BJ, Spaniel C et al. (2012) Stabilization of hepatitis C virus RNA by an Ago2-miR-122 complex. Proc Natl Acad Sci U S A 109: 941-946. doi:10.1073/pnas.1112263109. PubMed: 22215596.
20. Li Y, Masaki T, Yamane D, McGivern DR, Lemon SM (2013) Competing and noncompeting activities of miR-122 and the 5' exonuclease Xrn1 in regulation of hepatitis C virus replication. Proc Natl Acad Sci U S A 110: 1881-1886. doi:10.1073/pnas.1213515110. PubMed: 23248316.
21. Kutay H, Bai S, Datta J, Motiwala T, Pogribny I et al. (2006) Downregulation of miR-122 in the rodent and human hepatocellular carcinomas. J Cell Biochem 99: 671-678. doi:10.1002/jcb.20982. PubMed: 16924677.
22. Gramantieri L, Ferracin M, Fornari F, Veronese A, Sabbioni S et al. (2007) Cyclin G1 is a target of miR-122a, a microRNA frequently down-regulated in human hepatocellular carcinoma. Cancer Res 67: 6092-6099. doi:10.1158/0008-5472.CAN-06-4607. PubMed: 17616664.
23. Hou J, Lin L, Zhou W, Wang Z, Ding G et al. (2011) Identification of miRNomes in human liver and hepatocellular carcinoma reveals miR-199a/b-3p as therapeutic target for hepatocellular carcinoma. Cancer Cell 19: 232-243. doi:10.1016/j.ccr.2011.01.001. PubMed: 21316602.
24. Varnholt H, Drebber U, Schulze F, Wedemeyer I, Schirmacher P et al. (2008) MicroRNA gene expression profile of hepatitis C virus-associated hepatocellular carcinoma. Hepatology 47: 1223-1232. PubMed: 18307259.
25. Coulouarn C, Factor VM, Andersen JB, Durkin ME, Thorgeirsson SS (2009) Loss of miR-122 expression in liver cancer correlates with suppression of the hepatic phenotype and gain of metastatic properties. Oncogene 28: 3526-3536. doi:10.1038/onc.2009.211. PubMed: 19617899.
26. Bedossa P, Poynard T (1996) An algorithm for the grading of activity in chronic hepatitis C. The METAVIR Cooperative Study Group. Hepatology 24: 289-293. doi:10.1002/hep.510240201. PubMed: 8690394.
27. Desmet VJ, Gerber M, Hoofnagle JH, Manns M, Scheuer PJ (1994) Classification of Chronic Hepatitis: Diagnosis, Grading and Staging. Hepatology 19: 1513-1520. doi:10.1002/hep.1840190629. PubMed: 8188183.
28. Honda M, Sakai A, Yamashita T, Nakamoto Y, Mizukoshi E et al. (2010) Hepatic ISG expression is associated with genetic variation in interleukin 28B and the outcome of IFN therapy for chronic hepatitis C. Gastroenterology 139: 499-509. doi:10.1053/j.gastro.2010.04.049. PubMed: 20434452.
29. Schroeder A, Mueller O, Stocker S, Salowsky R, Leiber M et al. (2006) The RIN: an RNA integrity number for assigning integrity values to RNA measurements. BMC Mol Biol 7: 3. doi:10.1186/1471-2199-7-3. PubMed: 16448564.
30. Lanford RE, Guerra B, Lee H, Averett DR, Pfeiffer B et al. (2003) Antiviral effect and virus-host interactions in response to alpha interferon, gamma interferon, poly(i)-poly(c), tumor necrosis factor alpha, and ribavirin in hepatitis C virus subgenomic replicons. J Virol 77: 1092-1104. doi:10.1128/JVI.77.2.1092-1104.2003. PubMed: 12502825.
31. Nagaoki Y, Hyogo H, Aikata H, Tanaka M, Naeshiro N et al. (2012) Recent trend of clinical features in patients with hepatocellular carcinoma. Hepatol Res 42: 368-375. doi:10.1111/j.1872-034X.2011.00929.x. PubMed: 22151896.
32. Wang Y, Lu Y, Toh ST, Sung WK, Tan P et al. (2010) Lethal-7 is down-regulated by the hepatitis B virus x protein and targets signal transducer and activator of transcription 3. J Hepatol 53: 57-66. doi:10.1016/j.jhep.2009.12.043. PubMed: 20447714.
33. Hatziapostolou M, Polytarchou C, Aggelidou E, Drakaki A, Poultsides GA et al. (2011) An HNF4alpha-miRNA inflammatory feedback circuit regulates hepatocellular oncogenesis. Cell 147: 1233-1247. doi:10.1016/j.cell.2011.10.043. PubMed: 22153071.
34. Trebicka J, Anadol E, Elfimova N, Strack I, Roggendorf M et al. (2013) Hepatic and serum levels of miR-122 after chronic HCV-induced fibrosis. J Hepatol 58: 234-239. doi:10.1016/S0168-8278(13)60572-3. PubMed: 23085648.
35. Morita K, Taketomi A, Shirabe K, Umeda K, Kayashima H et al. (2011) Clinical significance and potential of hepatic microRNA-122 expression in hepatitis C. Liver Int 31: 474-484. doi:10.1111/j.1478-3231.2010.02433.x. PubMed: 21199296.
36. Sarasin-Filipowicz M, Krol J, Markiewicz I, Heim MH, Filipowicz W (2009) Decreased levels of microRNA miR-122 in individuals with hepatitis C responding poorly to interferon therapy. Nat Med 15: 31-33. doi:10.1038/nm.1902. PubMed: 19122656.
37. Tanaka Y, Nishida N, Sugiyama M, Kurosaki M, Matsuura K et al. (2009) Genome-wide association of IL28B with response to pegylated interferon-alpha and ribavirin therapy for chronic hepatitis C. Nat Genet 41: 1105-1109. doi:10.1038/ng.449. PubMed: 19749757.
38. Yoshizawa H (2002) Hepatocellular carcinoma associated with hepatitis C virus infection in Japan: projection to other countries in the foreseeable future. Oncology 62 Suppl 1: 8-17. doi:10.1159/000048270. PubMed: 11868791.
39. Sarasin-Filipowicz M, Oakeley EJ, Duong FH, Christen V, Terracciano L et al. (2008) Interferon signaling and treatment outcome in chronic hepatitis C. Proc Natl Acad Sci U S A 105: 7034-7039. doi:10.1073/pnas.0707882105. PubMed: 18467494.
40. Urban TJ, Thompson AJ, Bradrick SS, Fellay J, Schuppan D et al. (2010) IL28B genotype is associated with differential expression of intrahepatic interferon-stimulated genes in patients with chronic hepatitis C. Hepatology 52: 1888-1896. doi:10.1002/hep.23912. PubMed: 20931559.
41. Abe H, Hayes CN, Ochi H, Maekawa T, Tsuge M et al. (2011) IL28 variation affects expression of interferon stimulated genes and peg-interferon and ribavirin therapy. J Hepatol 54: 1094-1101. doi:10.1002/hep.24499. PubMed: 21145800.
42. Elyakim E, Sitbon E, Faerman A, Tabak S, Montia E et al. (2010) hsa-miR-191 is a candidate oncogene target for hepatocellular carcinoma therapy. Cancer Res 70: 8077-8087. doi:10.1158/0008-5472.CAN-10-1313. PubMed: 20924108.
43. Jangra RK, Yi M, Lemon SM (2010) miR-122 regulation of hepatitis C virus translation and infectious virus production. J Virol 84: 6615-6625. doi:10.1128/JVI.00417-10. PubMed: 20427538.
44. Fornari F, Gramantieri L, Giovannini C, Veronese A, Ferracin M et al. (2009) MiR-122/cyclin G1 interaction modulates p53 activity and affects doxorubicin sensitivity of human hepatocarcinoma cells. Cancer Res 69: 5761-5767. doi:10.1158/0008-5472.CAN-08-4797. PubMed: 19584283.
45. Tsai WC, Hsu SD, Hsu CS, Lai TC, Chen SJ et al. (2012) MicroRNA-122 plays a critical role in liver homeostasis and hepatocarcinogenesis. J Clin Invest 122: 2884-2897. doi:10.1172/JCI63455. PubMed: 22820290.
46. Hsu SH, Wang B, Kota J, Yu J, Costinean S et al. (2012) Essential metabolic, anti-inflammatory, and anti-tumorigenic functions of miR-122 in liver. J Clin Invest 122: 2871-2883. doi:10.1172/JCI63539. PubMed: 22820288.
47. Burns DM, D'Ambrogio A, Nottrott S, Richter JD (2011) CPEB and two poly(A) polymerases control miR-122 stability and p53 mRNA translation. Nature 473: 105-108. doi:10.1038/nature09908. PubMed: 21478871.

48. Lardizábal MN, Nocito AL, Daniele SM, Ornella LA, Palatnik JF et al. (2012) Reference genes for real-time PCR quantification of microRNAs and messenger RNAs in rat models of hepatotoxicity. PLOS ONE 7: e36323. doi:10.1371/journal.pone.0036323. PubMed: 22563491.
49. Norman KL, Sarnow P (2010) Modulation of hepatitis C virus RNA abundance and the isoprenoid biosynthesis pathway by microRNA miR-122 involves distinct mechanisms. J Virol 84: 666-670. doi: 10.1128/JVI.01156-09. PubMed: 19846523.
50. Li Y, Masaki T, Lemon SM (2013) miR-122 and the Hepatitis C RNA genome: More than just stability. RNA Biol 10: 919–24. PubMed: 23770926.
51. Janssen HL, Reesink HW, Lawitz EJ, Zeuzem S, Rodriguez-Torres M et al. (2013) Treatment of HCV Infection by Targeting MicroRNA. N Engl J Med, 368: 1685–94. PubMed: 23534542.
52. McGivern DR, Lemon SM (2011) Virus-specific mechanisms of carcinogenesis in hepatitis C virus associated liver cancer. Oncogene 30: 1969-1983. doi:10.1038/onc.2010.594. PubMed: 21258404.
53. Chen Y, Shen A, Rider PJ, Yu Y, Wu K et al. (2011) A liver-specific microRNA binds to a highly conserved RNA sequence of hepatitis B virus and negatively regulates viral gene expression and replication. FASEB J 25: 4511-4521. doi:10.1096/fj.11-187781. PubMed: 21903935.
54. Wang S, Qiu L, Yan X, Jin W, Wang Y et al. (2012) Loss of microRNA 122 expression in patients with hepatitis B enhances hepatitis B virus replication through cyclin G(1) -modulated P53 activity. Hepatology 55: 730-741. doi:10.1002/hep.24809. PubMed: 22105316.
55. Liu WH, Yeh SH, Chen PJ (2011) Role of microRNAs in hepatitis B virus replication and pathogenesis. Biochim Biophys Acta 1809: 678-685. doi:10.1016/j.bbagrm.2011.04.008. PubMed: 21565290.
56. Qiu L, Fan H, Jin W, Zhao B, Wang Y et al. (2010) miR-122-induced down-regulation of HO-1 negatively affects miR-122-mediated suppression of HBV. Biochem Biophys Res Commun 398: 771-777. doi:10.1016/j.bbrc.2010.07.021. PubMed: 20633528.
57. Liang Y, Shilagard T, Xiao SY, Snyder N, Lau D et al. (2009) Visualizing hepatitis C virus infections in human liver by two-photon microscopy. Gastroenterology 137: 1448-1458. doi:10.1053/j.gastro.2009.07.050. PubMed: 19632233.
58. Jung CJ, Iyengar S, Blahnik KR, Ajuha TP, Jiang JX et al. (2011) Epigenetic modulation of miR-122 facilitates human embryonic stem cell self-renewal and hepatocellular carcinoma proliferation. PLOS ONE 6: e27740. doi:10.1371/journal.pone.0027740. PubMed: 22140464.
59. Arai E, Ushijima S, Gotoh M, Ojima H, Kosuge T et al. (2009) Genome-wide DNA methylation profiles in liver tissue at the precancerous stage and in hepatocellular carcinoma. Int J Cancer 125: 2854-2862. doi: 10.1002/ijc.24708. PubMed: 19569176.
60. Jung JK, Park SH, Jang KL (2010) Hepatitis B virus X protein overcomes the growth-inhibitory potential of retinoic acid by downregulating retinoic acid receptor-beta2 expression via DNA methylation. J Gen Virol 91: 493-500. doi:10.1099/vir.0.015149-0. PubMed: 19828754.
61. Hsia CC, Thorgeirsson SS, Tabor E (1994) Expression of hepatitis B surface and core antigens and transforming growth factor-alpha in "oval cells" of the liver in patients with hepatocellular carcinoma. J Med Virol 43: 216-221. doi:10.1002/jmv.1890430304. PubMed: 7523580.
62. Pedersen IM, Cheng G, Wieland S, Volinia S, Croce CM et al. (2007) Interferon modulation of cellular microRNAs as an antiviral mechanism. Nature 449: 919-922. doi:10.1038/nature06205. PubMed: 17943132.
63. Wieland S, Thimme R, Purcell RH, Chisari FV (2004) Genomic analysis of the host response to hepatitis B virus infection. Proc Natl Acad Sci U S A 101: 6669-6674. doi:10.1073/pnas.0401771101. PubMed: 15100412.
64. Bigger CB, Guerra B, Brasky KM, Hubbard G, Beard MR et al. (2004) Intrahepatic gene expression during chronic hepatitis C virus infection in chimpanzees. J Virol 78: 13779-13792. doi:10.1128/JVI.78.24.13779-13792.2004. PubMed: 15564486.
65. Lanford RE, Guerra B, Bigger CB, Lee H, Chavez D et al. (2007) Lack of response to exogenous interferon-alpha in the liver of chimpanzees chronically infected with hepatitis C virus. Hepatology 46: 999-1008. doi:10.1002/hep.21776. PubMed: 17668868.

Research Article

EASL EUROPEAN ASSOCIATION FOR THE STUDY OF THE LIVER | JOURNAL OF HEPATOLOGY

The transcription factor SALL4 regulates stemness of EpCAM-positive hepatocellular carcinoma

Sha Sha Zeng[1], Taro Yamashita[1,2,*], Mitsumasa Kondo[1], Kouki Nio[1], Takehiro Hayashi[1], Yasumasa Hara[1], Yoshimoto Nomura[1], Mariko Yoshida[1], Tomoyuki Hayashi[1], Naoki Oishi[1], Hiroko Ikeda[3], Masao Honda[1], Shuichi Kaneko[1]

[1]*Department of Gastroenterology, Kanazawa University Hospital, Kanazawa, Ishikawa, Japan;* [2]*Department of General Medicine, Kanazawa University Hospital, Kanazawa, Ishikawa, Japan;* [3]*Department of Pathology, Kanazawa University Hospital, Kanazawa, Ishikawa, Japan*

Background & Aims: Recent evidence suggests that hepatocellular carcinoma can be classified into certain molecular subtypes with distinct prognoses based on the stem/maturational status of the tumor. We investigated the transcription program deregulated in hepatocellular carcinomas with stem cell features.

Methods: Gene and protein expression profiles were obtained from 238 (analyzed by microarray), 144 (analyzed by immunohistochemistry), and 61 (analyzed by qRT-PCR) hepatocellular carcinoma cases. Activation/suppression of an identified transcription factor was used to evaluate its role in cell lines. The relationship of the transcription factor and prognosis was statistically examined.

Results: The transcription factor SALL4, known to regulate stemness in embryonic and hematopoietic stem cells, was found to be activated in a hepatocellular carcinoma subtype with stem cell features. SALL4-positive hepatocellular carcinoma patients were associated with high values of serum alpha fetoprotein, high frequency of hepatitis B virus infection, and poor prognosis after surgery compared with SALL4-negative patients. Activation of SALL4 enhanced spheroid formation and invasion capacities, key characteristics of cancer stem cells, and up-regulated the hepatic stem cell markers *KRT19*, *EPCAM*, and *CD44* in cell lines. Knockdown of SALL4 resulted in the down-regulation of these stem cell markers, together with attenuation of the invasion capacity. The SALL4 expression status was associated with histone deacetylase activity in cell lines, and the histone deacetylase inhibitor successfully suppressed proliferation of SALL4-positive hepatocellular carcinoma cells.

Conclusions: SALL4 is a valuable biomarker and therapeutic target for the diagnosis and treatment of hepatocellular carcinoma with stem cell features.

Keywords: Cancer stem cell; Hepatocellular carcinoma; Gene expression profile; Chemosensitivity.

Received 15 March 2013; received in revised form 27 August 2013; accepted 28 August 2013; available online 6 September 2013

* Corresponding author. Address: Department of General Medicine/Gastroenterology, Kanazawa University Hospital, 13-1 Takara-Machi, Kanazawa, Ishikawa 920-8641, Japan. Tel.: +81 76 265 2042; fax: +81 76 234 4281.

E-mail address: taroy@m-kanazawa.jp (T. Yamashita).

Abbreviations: CSC, cancer stem cell; HCC, hepatocellular carcinoma; EpCAM, epithelial cell adhesion molecule; AFP, alpha fetoprotein; HpSC-HCC, hepatic stem cell-like HCC; MH-HCC, mature hepatocyte-like HCC; SALL4, Sal-like 4 (Drosophila); qRT-PCR, quantitative reverse transcription-polymerase chain reaction; HDAC, histone deacetylase; SAHA, suberoylanilide hydroxamic acid; SBHA, suberic bis-hydroxamic acid; NuRD, nucleosome remodeling and deacetylase.

Introduction

Cancer is a heterogeneous disease in terms of morphology and clinical behavior. This heterogeneity has traditionally been explained by the clonal evolution of cancer cells and the accumulation of serial stochastic genetic/epigenetic changes [1]. The alteration of the microenvironment by tumor stromal cells is also considered to contribute to the development of the heterogeneous nature of the tumor through the activation of various signaling pathways in cancer cells, including epithelial mesenchymal transition programs [2].

Recent evidence suggests that a subset of tumor cells with stem cell features, known as cancer stem cells (CSCs), are capable of self-renewal and can give rise to relatively differentiated cells, thereby forming heterogeneous tumor cell populations [3]. CSCs were also found to generate tumors more efficiently in immunodeficient mice than non-cancer stem cells in various solid tumors as well as hematological malignancies [4]. CSCs are also more metastatic and chemo/radiation-resistant than non-CSCs and are therefore considered to be a pivotal target for tumor eradication [5,6].

Hepatocellular carcinoma (HCC) is a leading cause of cancer death worldwide [7]. Recently, we proposed a novel HCC classification system based on the expression status of the hepatic stem/progenitor markers epithelial cell adhesion molecule (EpCAM) and alpha fetoprotein (AFP) [8]. EpCAM-positive ($^+$) AFP$^+$ HCC (hepatic stem cell-like HCC; HpSC-HCC) is characterized by an onset of disease at younger ages, activation of Wnt/β-catenin signaling, a high frequency of portal vein invasion and poor

prognosis after radical resection, compared with EpCAM$^-$ AFP$^-$ HCC (mature hepatocyte-like HCC; MH-HCC) [9]. *EPCAM* is a target gene of Wnt/β-catenin signaling, and EpCAM$^+$ HCC cells isolated from primary HCC and cell lines show CSC features including tumorigenicity, invasiveness, and resistance to fluorouracil [9,10]. Thus, EpCAM appears to be a potentially useful marker for the isolation of liver CSCs in HpSC-HCC. However, key transcriptional programs responsible for the maintenance of EpCAM$^+$ CSCs are still unclear.

In this study, we aimed to clarify the transcriptional programs deregulated in HpSC-HCC using a gene expression profiling approach. We found that the *SALL4* gene encoding Sal-like 4 (*Drosophila*) (SALL4), a zinc finger transcriptional activator and vertebrate orthologue of the *Drosophila* gene spalt (*sal*) [11], was up-regulated in HpSC-HCC. In adults, *SALL4* is known to be expressed in hematopoietic stem cells and their malignancies, but its role in HCC has not yet been fully elucidated [12–14]. We therefore investigated the role of SALL4 in the regulation and maintenance of EpCAM$^+$ HCC.

Materials and methods

Clinical HCC specimens

A total of 144 HCC tissues and adjacent non-cancerous liver tissues were obtained from patients who underwent hepatectomy for HCC treatment from 2002 to 2010 at Kanazawa University Hospital, Kanazawa, Japan. These samples were formalin-fixed and paraffin-embedded, and used for immunohistochemistry (IHC). A further 61 HCC samples were obtained from patients who underwent hepatectomy from 2008 to 2011; these were freshly snap-frozen in liquid nitrogen and used for RNA analysis. Of these 61 HCCs, 8 and 36 cases were defined as HpSC-HCC and MH-HCC, respectively, according to previously described criteria [8].

27 HCC cases were included in both the IHC cohort (n = 144) and quantitative reverse transcription-polymerase chain reaction (qRT-PCR) cohort (n = 61), and SALL4 gene and protein expression were compared between these cases. An additional fresh HpSC-HCC sample was obtained from a surgically resected specimen and immediately used for preparation of a single-cell suspension. All experimental and tissue acquisition procedures were approved by the Ethics Committee and the Institutional Review Board of Kanazawa University Hospital. All patients provided written informed consent.

Microarray analysis

Detailed information on microarray analysis is available in the Supplementary Materials and methods.

Cell culture and reagents

Human liver cancer cell lines HuH1, HuH7, HLE, and HLF were obtained from the Japanese Collection of Research Bioresources (JCRB), and Hep3B and SK-Hep-1 were obtained from the American Type Culture Collection (ATCC). Single-cell suspensions of primary HCC tissue were prepared as described previously [15]. Detailed information is available in the Supplementary Materials and methods. The histone deacetylase (HDAC) inhibitor suberic bis-hydroxamic acid (SBHA) and suberoylanilide hydroxamic acid (SAHA) were obtained from Cayman Chemical (Ann Arbor, MI). Plasmid constructs pCMV6-SALL4 (encoding *SALL4A*), pCMV6-SALL4-GFP, and 29mer shRNA constructs against human SALL4 (No. 7412) were obtained from OriGene Technologies, Inc. (Rockville, MD). These constructs were transfected using Lipofectamine 2000 (Life Technologies, Carlsbad, CA) according to the manufacturer's protocol.

Western blotting

Whole cell lysates were prepared using RIPA lysis buffer. Nuclear and cytoplasmic proteins were extracted using NE-PER Nuclear and Cytoplasmic Extraction Reagents (Pierce Biotechnology Inc., Rockford, IL). Mouse monoclonal antibody to human Sall4 clone 6E3 (Abnova, Walnut, CA), rabbit polyclonal antibodies to human Lamin B1 (Cell Signaling Technology Inc., Danvers, MA), and mouse monoclonal anti-β-actin antibody (Sigma-Aldrich, St. Louis, MO) were used. Immune complexes were visualized by enhanced chemiluminescence (Amersham Biosciences Corp., Piscataway, NJ) as described previously [15,16].

Quantitative reverse transcription-polymerase chain reaction (qRT-PCR)

Detailed information on qRT-PCR is available in the Supplementary Materials and methods.

IHC and immunofluorescence (IF) analyses

IHC was performed using an Envision+ kit (Dako, Carpinteria, CA) according to the manufacturer's instructions. Anti-SALL4 monoclonal antibody 6E3 (Abnova, Walnut, CA), anti-EpCAM monoclonal antibody VU-1D9 (Oncogene Research Products, San Diego, CA), and anti-CK19 monoclonal antibody RCK108 (Dako Japan, Tokyo, Japan) were used for detecting SALL4, EpCAM, and CK19, respectively. Anti-Sall4 rabbit polyclonal antibodies (ab29112) (Abnova) and vector red (Vector Laboratories Inc., Burlingame, CA) were used for double color IHC analysis. Samples with >5% positive staining in a given area were considered to be positive for a particular antibody. For IF analyses, Alexa 488 fluorescein isothiocyanate (FITC)-conjugated anti-mouse immunoglobulin G (IgG) (Life Technologies) was used as a secondary antibody.

Cell proliferation, spheroid formation, invasion, and HDAC activity assay

Detailed information on this topic is available in the Supplementary Materials and methods.

Statistical analyses

Student's *t* tests were performed with GraphPad Prism software 5.0 (GraphPad Software, San Diego, CA) to compare various test groups assayed by cell proliferation assays and qRT-PCR analysis. Spearman's correlation analysis and Kaplan-Meier survival analysis were also performed with GraphPad Prism software 5.0 (GraphPad Software).

Results

Activation of SALL4 in HpSC-HCC

To elucidate the transcriptional programs deregulated in HpSC-HCC, we performed class-comparison analyses and identified 793 genes showing significant differences in differential expression between HpSC-HCC (n = 60) and MH-HCC (n = 96) (p <0.001), as previously described [9]. Of them, 455 genes were specifically up-regulated in HpSC-HCC, and we performed transcription factor analysis using this gene set to identify their transcriptional regulators by MetaCore software. We identified four transcription factor genes, *SALL4*, *NFYA*, *TP53*, and *SP1*, that were potentially activated in HpSC-HCC (Fig. 1A). Involvement of *TP53* and *SP1* in the stemness of HCC has previously been described [17,18], but the roles of *SALL4* and *NFYA* were unclear.

We investigated the interaction networks affected by *SALL4* and *NFYA* using the MetaCore dataset. We showed that *SALL4* might be a regulator of Akt signaling (*SP1*), Wnt signaling (*TCF7L2*), and epigenetic modification (*JARID2*, *DMRT1*, *DNMT3B*) [19], and could potentially regulate two other transcriptional regulators, *SP1* and *NFYA*, through Akt and Myb signaling pathways (Fig. 1B). As a recent study indicated that *SALL4* is a direct target of the Wnt signaling pathway [20], which is dominantly activated in HpSC-HCC [9], we focused on the expression of *SALL4* in HpSC-HCC, and confirmed its up-regulation in HpSC-HCC compared

A

Transcription factors	*p* value	z-score
SALL4	0.0005708	3.958
NFYA	0.002483	3.267
TP53	3.923E-05	4.25
SP1	2.917E-11	6.942

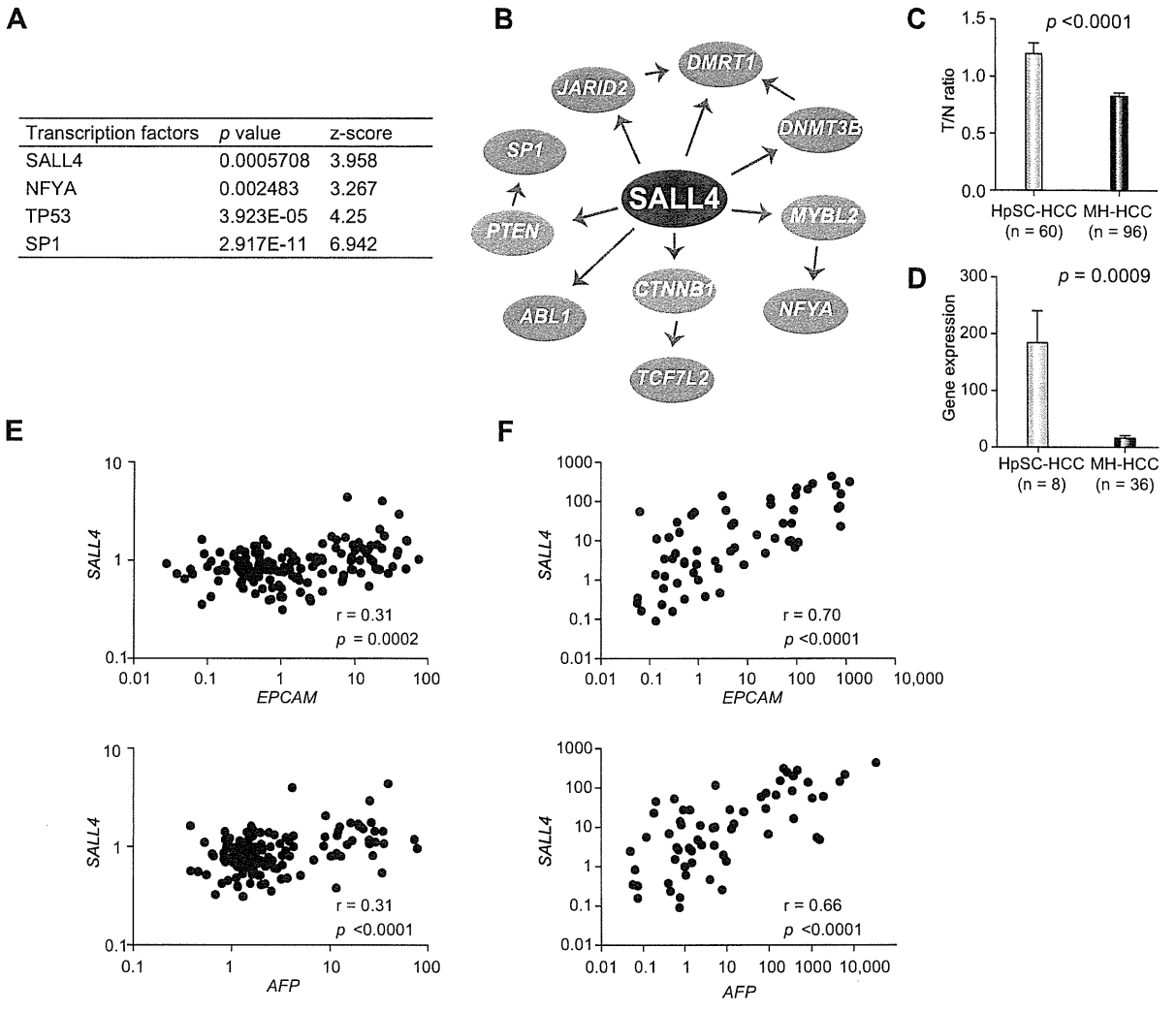

Fig. 1. Transcription factors potentially activated in HpSC-HCC. (A) Transcription factor analysis. Transcription factors regulating genes up-regulated in HpSC-HCC are listed with their *p* values and z-scores as calculated by MetaCore software. (B) Interaction network analysis. Seven genes (*ABL1*, *DMRT1*, *DNMT3B*, *JARID2*, *NFYA*, *SP1*, and *TCF7L2*, indicated in orange) shown to be up-regulated in HpSC-HCC were identified as potential target genes regulated by *SALL4* (indicated in red). (C) *SALL4* gene expression evaluated by microarray analysis. Tumor/non-tumor (T/N) ratios of microarray data in HpSC-HCC (n = 60) and MH-HCC (n = 96). (D) *SALL4* gene expression evaluated by qRT-PCR. Gene expression of *SALL4* in HpSC-HCC (n = 8) and MH-HCC (n = 36) samples. (E) Scatter plot analysis. Gene expression levels of *EPCAM* (upper panel) and *AFP* (lower panel) were positively correlated with those of *SALL4* in microarray data (n = 238, T/N ratios), as shown by Spearman's correlation coefficients. (F) Scatter plot analysis. Gene expression levels of *EPCAM* (upper panel) and *AFP* (lower panel) were positively correlated with those of *SALL4* in qRT-PCR data (n = 61), as shown by Spearman's correlation coefficients. (This figure appears in colour on the web.)

with MH-HCC as evaluated by microarray data (Fig. 1C). We validated this using an independent HCC cohort evaluated by qRT-PCR (Fig. 1D). We further examined the expression of *SALL4*, *EPCAM*, and *AFP* using microarray data of 238 HCC cases (Fig. 1E) and qRT-PCR data of 61 HCC cases (Fig. 1F). For the tumor/non-tumor ratios, we identified a weak positive correlation between *SALL4* and *EPCAM* (r = 0.31, $p < 0.0001$) and between *SALL4* and *AFP* (r = 0.31, $p = 0.0003$) in the microarray cohort. We further evaluated expression of these genes in HCC tissues by qRT-PCR, and we validated the strong positive correlation between *SALL4* and *EPCAM* (r = 0.70, $p < 0.0001$) and between *SALL4* and AFP (r = 0.66, $p < 0.0001$) in the independent cohort.

Next we performed IHC analysis of 144 HCC cases surgically resected at Kanazawa University Hospital. We first confirmed the nuclear accumulation of SALL4 stained by an anti-human SALL4 antibody (Fig. 2A). We further confirmed the concordance of SALL4 protein expression evaluated by IHC, and *SALL4* gene expression evaluated by qRT-PCR using the same samples (Fig. 2B). We detected the nuclear expression of SALL4 in 43 of 144 HCC cases (Table 1). After evaluating the clinicopathological characteristics of SALL4-positive and -negative HCC cases, we identified that SALL4-positive HCCs were associated with a significantly high frequency of hepatitis B virus (HBV) infection and significantly high serum AFP values. We further identified that

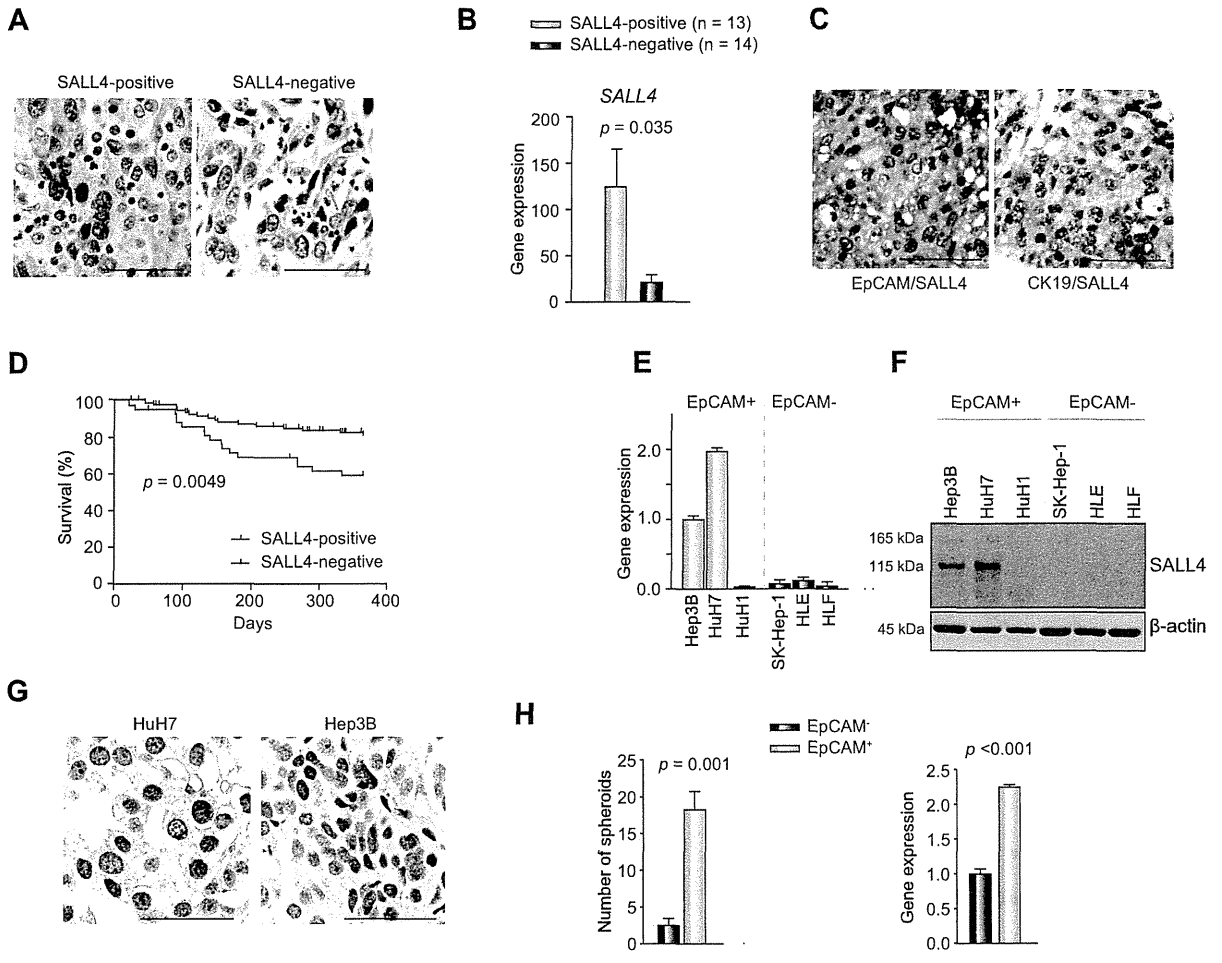

Fig. 2. *SALL4* expression in human primary HCCs and cell lines. (A) Representative images of SALL4-positive and -negative HCC immunostaining (scale bar, 100 μm). (B) Gene expression of *SALL4* in SALL4-positive (n = 13) and -negative HCCs (n = 14) as shown by IHC (mean ± SD). (C) Double color IHC analysis of HCC stained with anti-SALL4 and anti-EpCAM or anti-CK19 antibodies (scale bar, 100 μm). (D) Kaplan-Meier survival analysis with Log-rank. Recurrence-free survival of SALL4-positive (n = 43) and -negative (n = 101) HCCs was analyzed. (E) *SALL4* expression in EpCAM$^+$ (Hep3B, HuH7, and HuH1) and EpCAM$^-$ (SK-Hep-1, HLE, and HLF) HCC cell lines evaluated by qRT-PCR. (F) SALL4 expression in EpCAM$^+$ and EpCAM$^-$ HCC cell lines evaluated by Western blotting. (G) IHC analysis of SALL4 expression in subcutaneous tumors obtained from EpCAM$^+$ (HuH7 and Hep3B) HCC cell lines xenografted in NOD/SCID mice. (H) Spheroid formation capacity of sorted EpCAM$^+$ and EpCAM$^-$ cells obtained from a primary HCC. Number of spheroids obtained from 2000 sorted cells is indicated (n = 3, mean ± SD). Gene expression of *SALL4* in sorted EpCAM$^+$ and EpCAM$^-$ cells obtained from a primary HCC (n = 3, mean ± SD). (This figure appears in colour on the web.)

SALL4-positive HCCs were associated with expression of the hepatic stem cell markers EpCAM and CK19. Co-expression of SALL4, EpCAM, and CK19 was confirmed by double color IHC analysis (Fig. 2C). Evaluation of the survival outcome of these surgically resected HCC cases by Kaplan-Meier survival analysis indicated that SALL4-positive HCCs were associated with significantly lower recurrence-free survival outcomes within one year compared with SALL4-negative HCCs ($p = 0.0049$) (Fig. 2D).

Because *SALL4* expression was positively correlated with EpCAM and AFP expression in primary HCC cases, we evaluated the expression of SALL4 in EpCAM$^+$ AFP$^+$ and EpCAM$^-$ AFP$^-$ HCC cell lines. Consistent with the primary HCC data, two of three EpCAM$^+$ AFP$^+$ HCC cell lines (Hep3B and HuH7) abundantly expressed SALL4, as shown by qRT-PCR (Fig. 2E) and Western blotting (Fig. 2F). We identified the expression of two isoforms of SALL4 proteins with molecular weights of 165 kDa (SALL4A) and 115 kDa (SALL4B), and SALL4B was found to be the dominant endogenous isoform in HCC cell lines. All EpCAM$^-$ AFP$^-$ HCC cell lines (SK-Hep-1, HLE, and HLF) and one EpCAM$^+$ AFP$^+$ cell line (HuH1) did not express SALL4. Nuclear accumulation of SALL4 in Hep3B and HuH7 cells was confirmed by IHC using subcutaneous tumors developed in xenotransplanted NOD/SCID mice (Fig. 2G). We further evaluated the expression of *EPCAM* and *SALL4* using single cell suspensions derived from a surgically resected primary HCC. EpCAM$^+$ and EpCAM$^-$ cells were separated by magnetic beads, and we revealed a strong spheroid formation capacity of sorted EpCAM$^+$ cells compared with EpCAM$^-$ cells (Fig. 2H, left panel). Interestingly, when comparing the expression of *SALL4* in these sorted cells, we identified a high expression of *SALL4* in sorted EpCAM$^+$ cells compared with EpCAM$^-$ cells (Fig. 2H, right panel), indicating that SALL4 is activated in EpCAM$^+$ liver CSCs.

Table 1. Clinicopathological characteristics of SALL4-positive and -negative HCC cases used for IHC analyses.

Parameters	SALL4-positive (n = 43)	SALL4-negative (n = 101)	*p* value*
Age (yr, mean ± SE)	60.8 ± 1.8	64.6 ± 1.0	0.13
Sex (male/female)	27/16	70/18	0.06
Etiology (HBV/HCV/B + C/other)	21/14/0/8	20/63/3/15	0.0014
Liver cirrhosis (yes/no)	21/22	61/40	0.27
AFP (ng/ml, mean ± SE)	13,701 ± 9292	175.5 ± 55.0	<0.0001
Histological grade**			
I-II	3	18	
II-III	33	68	
III-IV	7	15	0.24
Tumor size (<3 cm/>3 cm)	17/26	57/44	0.071
EpCAM (positive/negative)	27/16	29/72	0.0002
CK19 (positive/negative)	12/31	12/89	0.027

*Mann-Whitney U-test or χ^2 test.
**Edmondson-Steiner.

SALL4 regulates stemness of HpSC-HCC

To explore the role of SALL4 in HpSC-HCC, we evaluated the effect of its overexpression in HuH1 cells which showed little expression of SALL4 irrespective of EpCAM$^+$ and AFP$^+$ HpSC-HCC phenotype. We transfected plasmid constructs encoding SALL4 (pCMV6-SALL4) or control (pCMV7), and we similarly identified the expression of two isoforms by using this construct (Fig. 3A). Evaluation of the subcellular localization of GFP-tagged SALL4 (pCMV6-SALL4-GFP) showed that it could be detected in both the cytoplasm and nucleus (Fig. 3B). We observed strong up-regulation of the hepatic stem cell marker *KRT19*, modest up-regulation of *EPCAM* and *CD44*, and down-regulation of the mature hepatocyte marker *ALB* in HuH1 cells transfected with pCMV6-SALL4 compared with the control (Fig. 3C). Up-regulation of CK19 by SALL4 overexpression was also confirmed at the protein level by IF analysis (Fig. 3D). Phenotypically, SALL4 overexpression in HuH1 cells resulted in the significant activation of spheroid formation and invasion capacities with activation of *SNAI1*, which induces epithelial-mesenchymal transition, compared with the control (Fig. 3E and F, Supplementary Fig. 1A).

We further investigated the effect of SALL4 knockdown in HuH7 cells, which intrinsically expressed high levels of SALL4. Expression of *SALL4* was decreased to 50% in HuH7 cells transfected with SALL4 sh-RNA compared with the control when evaluated by qRT-PCR (Fig. 4A). However, the reduction of SALL4 protein was more evident when evaluated by Western blotting, suggesting that this sh-RNA construct might work at the translational as well as the transcriptional level (Fig. 4B). Knock down of *SALL4* resulted in a compromised invasion capacity and spheroid formation capacity with decreased expression of *EPCAM* and *CD44* in HuH7 cells (Fig. 4C and D, Supplementary Fig. 1B and C).

SALL4 and HDAC activity in HpSC-HCC

The above data suggested that SALL4 is a good target and biomarker for the diagnosis and treatment of HpSC-HCCs. However, it is difficult to directly target SALL4 as no studies have investigated the inhibition of its transcription using chemical or other approaches [21]. We therefore re-investigated the interaction networks associated with *SALL4*, and found that SALL4 activation appeared to induce epigenetic modification (Fig. 1B). In particular, a recent study suggested that SALL4 forms a nucleosome remodeling and deacetylase (NuRD) complex with HDACs and potentially regulates HDAC activity [22]. We therefore confirmed that *SALL4* knock down resulted in the reduced activity of total HDAC in HuH7 cells (Fig. 4E). We also evaluated the effect of the overexpression of SALL4 in HuH1 and HLE cells, which do not express SALL4 endogenously, and SALL4 overexpression was found to result in a modest increase of HDAC activity and mild enhancement of chemosensitivity to an HDAC inhibitor SBHA in both cell lines (Supplementary Fig. 2A and B). We further investigated HDAC activity in two SALL4-positive (Hep3B, HuH7) and two SALL4-negative (HLE, HLF) HCC cell lines. Interestingly, high HDAC activities were detected in SALL4-positive compared with SALL4-negative HCC cell lines (Fig. 4F). The HDAC inhibitor SBHA was found to inhibit proliferation of SALL4-positive HCC cell lines at a concentration of 10 μM. By contrast, SBHA had little effect on the proliferation of SALL4-negative HCC cell lines at this concentration (Fig. 4G). SBHA treatment suppressed the expression of SALL4 gene/protein expression in SALL4-positive HuH7 and Hep3B cell lines (Supplementary Fig. 3A and B). We further investigated the effect of SAHA, an additional HDAC inhibitor, in these HCC cell lines, and SAHA was found to more efficiently suppress the cell proliferation of SALL4-positive cell lines compared with SALL4-negative cell lines (Supplementary Fig. 3C).

Taken together, our data suggest a pivotal role for the transcription factor SALL4 in regulating the stemness of HpSC-HCC. SALL4 was detected in HpSC-HCCs with poor prognosis, and inactivation of SALL4 resulted in a reduced invasion/spheroid formation capacity and decreased expression of hepatic stem cell markers. The HDAC inhibitors inhibited proliferation of SALL4-positive HCC cell lines with a reduction of SALL4 gene/protein expression, suggesting their potential in the treatment of SALL4-positive HpSC-HCC.

Discussion

Stemness traits in cancer cells are currently of great interest because they may explain the clinical outcome of patients according to the malignant nature of their tumor. Recently, we

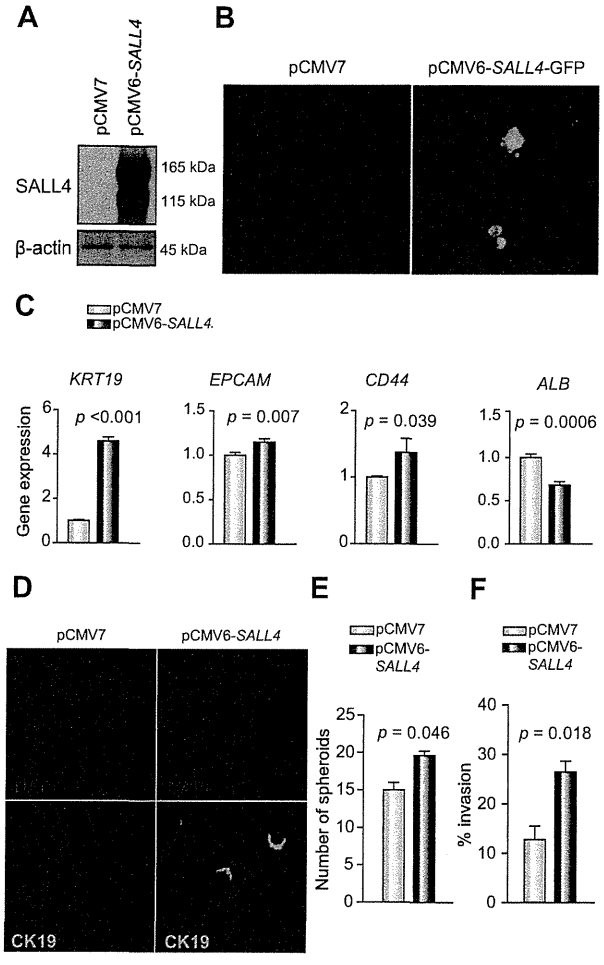

Fig. 3. Effect of SALL4 overexpression. (A) Western blots of cell lysates with anti-SALL4 antibodies. HuH1 cells were transfected with pCMV7 or pCMV6-*SALL4* and incubated for 72 h. (B) IF analysis of HuH1 cells transfected with pCMV7 or pCMV6-*SALL4* and incubated for 72 h. (C) qRT-PCR analysis of *KRT19*, *EPCAM*, *CD44*, and *ALB* in HuH1 cells transfected with pCMV7 or pCMV6-*SALL4* and incubated for 48 h. (D) IF analysis of HuH1 cells transfected with pCMV7 or pCMV6-*SALL4*, incubated for 72 h and stained with anti-CK19 antibodies, evaluated by the confocal laser scanning microscopy. (E) Spheroid formation assay of HuH1 cells transfected with pCMV7 or pCMV6-*SALL4*. Number of spheroids obtained from 2000 cells is indicated (n = 3, mean ± SD). (F) Invasion assay of HuH1 cells transfected with pCMV7 or pCMV6-*SALL4* (n = 3, mean ± SD). (This figure appears in colour on the web.)

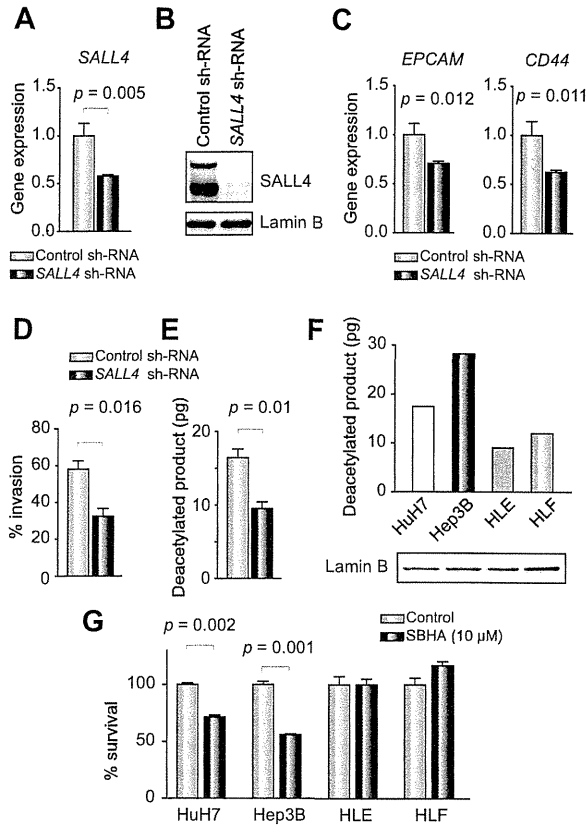

Fig. 4. Effect of *SALL4* knockdown and HDAC activity. (A) qRT-PCR analysis of *SALL4* in HuH7 cells transfected with control or *SALL4* sh-RNAs (n = 3, mean ± SD). (B) Western blots of lysates obtained from HuH7 cells transfected with control or *SALL4* sh-RNAs with anti-SALL4 antibodies. (C) qRT-PCR analysis of *EPCAM* and *CD44* in HuH7 cells transfected with control or *SALL4* sh-RNAs (n = 3, mean ± SD). (D) Invasion assay of HuH7 cells transfected with control or *SALL4* sh-RNAs (n = 3, mean ± SD). (E) HDAC activity of nuclear extracts obtained from HuH7 cells transfected with control or *SALL4* sh-RNAs. (F) HDAC activity of nuclear extracts obtained from each cell line. HDAC activity was measured in duplicate and average amounts of deacetylated products are indicated (upper panel). Lamin B included in the nuclear extracts loaded for HDAC activity assays was measured by Western blotting (lower panel). (G) Cell proliferation assay of HCC cell lines. Each cell line was treated with control DMSO or 10 μM SBHA and cultured for 72 h (n = 4, mean ± SD).

proposed an HCC classification system based on the stem/maturation status of the tumor by EpCAM and AFP expression status [8]. These HCC subtypes showed distinct gene expression patterns with features resembling particular stages of liver lineages. Among them, HpSC-HCC was characterized by a highly invasive nature, chemoresistance to fluorouracil, and poor prognosis after radical resection, warranting the development of a novel therapeutic approach against this HCC subtype [9].

In this study, we showed that the transcription factor SALL4 was activated in HpSC-HCC and that SALL4 might regulate HCC stemness, as characterized by the activation of EpCAM, CK19, and CD44 with highly tumorigenic and invasive natures. Furthermore, we identified that SALL4-positive HCC cell lines tended to show high HDAC activity and chemosensitivity to the HDAC inhibitors SBHA and SAHA. This study reveals for the first time the utility of SBHA for the treatment of HCC with stem cell features.

SALL4 is a zinc finger transcription factor originally cloned based on sequence homology to *Drosophila sal* [11]. *SALL4* mutations are associated with the Okihiro syndrome, a human disease involving multiple organ defects [23,24]. SALL4 plays a fundamental role in the maintenance of embryonic stem cells, potentially through interaction with Oct4, Sox2, and Nanog [25–30]. Furthermore, knockdown of SALL4 significantly reduces the efficiency of induced pluripotent stem cell generation [31]. *SALL4* is also expressed in hematopoietic stem cells and leukemia cells, where it regulates their maintenance [14,32]. SALL4 is known to encode two isoforms (SALL4A and SALL4B), and a recent study

suggested the important role of SALL4B on maintaining the stemness of embryonic stem cells [25]. Interestingly, our data indicated that SALL4B is also a dominant form in HpSC-HCC cell lines. It is unclear how SALL4 isoform expression is regulated in cancer, and future studies are required to explore the mechanisms of SALL4 isoform regulation.

In the liver, SALL4 is expressed in fetal hepatic stem/progenitors but not in adult hepatocytes, and a mouse study demonstrated that inhibition of SALL4 in hepatic stem/progenitors contributes to their differentiation [33]. Interestingly, recent studies indicated that AFP-producing gastric cancer expresses SALL4, suggesting that SALL4 might play a role in the hepatoid differentiation of gastric cancer [34]. Consistently, our data indicated a positive correlation between *SALL4*, *AFP*, and *EPCAM* expression in two independent HCC cohorts. Strikingly, SALL4 was recently shown to be expressed in a subset of human liver cancers with poor prognoses, while modification of SALL4 expression resulted in the alteration of cell proliferation *in vitro* and tumor growth *in vivo*, consistent with our current study [35]. A recent study reported the expression of SALL4 in 46% of HCC cases, which is almost comparable to our present study [36]. Furthermore, a very recent study of two independent large cohorts demonstrated that SALL4 is a marker for a progenitor subclass of HCC with an aggressive phenotype [37]. It is still unclear how SALL4 expression is regulated and which target genes are directly activated by SALL4 binding. Future studies using next generation sequencing are required to fully understand the mechanisms of SALL4 regulation of HCC stemness.

In this study, we demonstrated that SALL4-positive HCC cell lines have high HDAC activity and chemosensitivity against the HDAC inhibitors SBHA and SAHA compared with SALL4-negative HCC cell lines. SALL4 was recently found to directly connect with the epigenetic modulator NuRD complex [22], thereby possibly affecting the histone modification associated with stemness. The NuRD complex is a multiunit chromatin remodeling complex containing chromodomain-helicase-DNA-binding proteins and HDACs that regulate histone deacetylation [38]. Its role in cancer is still controversial, while its function in HCC has not yet been determined.

Our data suggest that SALL4 plays a role in controlling HDAC activity and contributing to the maintenance of HCC with stem cell features. Consistently, HDAC inhibitors might be useful for the eradication of SALL4-positive HCC cells through their inhibitory effects on histone deacetylation by NuRD [39]. Encouragingly, a recent study demonstrated the utility of a SALL4-binding peptide to inhibit its binding to phosphatase and tensin homolog deleted on chromosome 10 (PTEN) through interaction with HDAC, thereby targeting leukemia cells [21]. Further studies are required to understand the relationship between SALL4, the NuRD complex, and the maintenance of stemness in HCC.

Financial support

This study was supported by a Grant-in-Aid from the Ministry of Education, Culture, Sports, Science and Technology, Japan (23590967), a grant from the Japanese Society of Gastroenterology, a grant from the Ministry of Health, Labour and Welfare, and a grant from the National Cancer Center Research and Development Fund (23-B-5), Japan.

Conflict of interest

The authors who have taken part in this study declared that they do not have anything to disclose regarding funding or conflict of interest with respect to this manuscript.

Acknowledgments

We thank Ms. Masayo Baba and Ms. Nami Nishiyama for excellent technical assistance.

Supplementary data

Supplementary data associated with this article can be found, in the online version, at http://dx.doi.org/10.1016/j.jhep.2013.08.024.

References

[1] Nowell PC. The clonal evolution of tumor cell populations. Science 1976;194:23–28.
[2] Hanahan D, Weinberg RA. Hallmarks of cancer: the next generation. Cell 2011;144:646–674.
[3] Jordan CT, Guzman ML, Noble M. Cancer stem cells. N Engl J Med 2006;355:1253–1261.
[4] Clarke MF, Dick JE, Dirks PB, Eaves CJ, Jamieson CH, Jones DL, et al. Cancer stem cells–perspectives on current status and future directions: AACR Workshop on cancer stem cells. Cancer Res 2006;66:9339–9344.
[5] Dean M, Fojo T, Bates S. Tumour stem cells and drug resistance. Nat Rev Cancer 2005;5:275–284.
[6] Visvader JE, Lindeman GJ. Cancer stem cells in solid tumours: accumulating evidence and unresolved questions. Nat Rev Cancer 2008;8:755–768.
[7] Jemal A, Bray F, Center MM, Ferlay J, Ward E, Forman D. Global cancer statistics. CA Cancer J Clin 2011;61:69–90.
[8] Yamashita T, Forgues M, Wang W, Kim JW, Ye Q, Jia H, et al. EpCAM and alpha-fetoprotein expression defines novel prognostic subtypes of hepatocellular carcinoma. Cancer Res 2008;68:1451–1461.
[9] Yamashita T, Ji J, Budhu A, Forgues M, Yang W, Wang HY, et al. EpCAM-positive hepatocellular carcinoma cells are tumor-initiating cells with stem/progenitor cell features. Gastroenterology 2009;136:1012–1024.
[10] Yamashita T, Budhu A, Forgues M, Wang XW. Activation of hepatic stem cell marker EpCAM by Wnt-beta-catenin signaling in hepatocellular carcinoma. Cancer Res 2007;67:10831–10839.
[11] de Celis JF, Barrio R. Regulation and function of spalt proteins during animal development. Int J Dev Biol 2009;53:1385–1398.
[12] Aguila JR, Liao W, Yang J, Avila C, Hagag N, Senzel L, et al. SALL4 is a robust stimulator for the expansion of hematopoietic stem cells. Blood 2011;118:576–585.
[13] Yang J, Chai L, Gao C, Fowles TC, Alipio Z, Dang H, et al. SALL4 is a key regulator of survival and apoptosis in human leukemic cells. Blood 2008;112:805–813.
[14] Yang J, Chai L, Liu F, Fink LM, Lin P, Silberstein LE, et al. Bmi-1 is a target gene for SALL4 in hematopoietic and leukemic cells. Proc Natl Acad Sci U S A 2007;104:10494–10499.
[15] Yamashita T, Honda M, Nio K, Nakamoto Y, Takamura H, Tani T, et al. Oncostatin m renders epithelial cell adhesion molecule-positive liver cancer stem cells sensitive to 5-fluorouracil by inducing hepatocytic differentiation. Cancer Res 2010;70:4687–4697.
[16] Yamashita T, Honda M, Takatori H, Nishino R, Minato H, Takamura H, et al. Activation of lipogenic pathway correlates with cell proliferation and poor prognosis in hepatocellular carcinoma. J Hepatol 2009;50:100–110.
[17] Woo HG, Wang XW, Budhu A, Kim YH, Kwon SM, Tang ZY, et al. Association of TP53 mutations with stem cell-like gene expression and survival of patients with hepatocellular carcinoma. Gastroenterology 2011;140:1063–1070.
[18] Ji J, Wang XW. Clinical implications of cancer stem cell biology in hepatocellular carcinoma. Semin Oncol 2012;39:461–472.

[19] Yang J, Corsello TR, Ma Y. Stem cell gene SALL4 suppresses transcription through recruitment of DNA methyltransferases. J Biol Chem 2012;287: 1996–2005.
[20] Bohm J, Sustmann C, Wilhelm C, Kohlhase J. SALL4 is directly activated by TCF/LEF in the canonical Wnt signaling pathway. Biochem Biophys Res Commun 2006;348:898–907.
[21] Gao C, Dimitrov T, Yong KJ, Tatetsu H, Jeong HW, Luo HR, et al. Targeting transcription factor SALL4 in acute myeloid leukemia by interrupting its interaction with an epigenetic complex. Blood 2013;121:1413–1421.
[22] Lu J, Jeong HW, Kong N, Yang Y, Carroll J, Luo HR, et al. Stem cell factor SALL4 represses the transcriptions of PTEN and SALL1 through an epigenetic repressor complex. PLoS One 2009;4:e5577.
[23] Al-Baradie R, Yamada K, St Hilaire C, Chan WM, Andrews C, McIntosh N, et al. Duane radial ray syndrome (Okihiro syndrome) maps to 20q13 and results from mutations in SALL4, a new member of the SAL family. Am J Hum Genet 2002;71:1195–1199.
[24] Kohlhase J, Heinrich M, Schubert L, Liebers M, Kispert A, Laccone F, et al. Okihiro syndrome is caused by SALL4 mutations. Hum Mol Genet 2002;11:2979–2987.
[25] Rao S, Zhen S, Roumiantsev S, McDonald LT, Yuan GC, Orkin SH. Differential roles of Sall4 isoforms in embryonic stem cell pluripotency. Mol Cell Biol 2010;30:5364–5380.
[26] Tanimura N, Saito M, Ebisuya M, Nishida E, Ishikawa F. Stemness-related factor sall4 interacts with transcription factors oct-3/4 and sox2 and occupies oct-sox elements in mouse embryonic stem cells. J Biol Chem 2013;288:5027–5038.
[27] Wu Q, Chen X, Zhang J, Loh YH, Low TY, Zhang W, et al. Sall4 interacts with nanog and co-occupies nanog genomic sites in embryonic stem cells. J Biol Chem 2006;281:24090–24094.
[28] Yang J, Chai L, Fowles TC, Alipio Z, Xu D, Fink LM, et al. Genome-wide analysis reveals Sall4 to be a major regulator of pluripotency in murine-embryonic stem cells. Proc Natl Acad Sci U S A 2008;105:19756–19761.
[29] Yang J, Gao C, Chai L, Ma Y. A novel SALL4/OCT4 transcriptional feedback network for pluripotency of embryonic stem cells. PLoS One 2010;5:e10766.
[30] Zhang J, Tam WL, Tong GQ, Wu Q, Chan HY, Soh BS, et al. Sall4 modulates embryonic stem cell pluripotency and early embryonic development by the transcriptional regulation of Pou5f1. Nat Cell Biol 2006;8:1114–1123.
[31] Tsubooka N, Ichisaka T, Okita K, Takahashi K, Nakagawa M, Yamanaka S. Roles of Sall4 in the generation of pluripotent stem cells from blastocysts and fibroblasts. Genes Cells 2009;14:683–694.
[32] Yang J, Liao W, Ma Y. Role of SALL4 in hematopoiesis. Curr Opin Hematol 2012;19:287–291.
[33] Oikawa T, Kamiya A, Kakinuma S, Zeniya M, Nishinakamura R, Tajiri H, et al. Sall4 regulates cell fate decision in fetal hepatic stem/progenitor cells. Gastroenterology 2009;136:1000–1011.
[34] Ikeda H, Sato Y, Yoneda N, Harada K, Sasaki M, Kitamura S, et al. Alpha-Fetoprotein-producing gastric carcinoma and combined hepatocellular and cholangiocarcinoma show similar morphology but different histogenesis with respect to SALL4 expression. Hum Pathol 2012;43:1955–1963.
[35] Oikawa T, Kamiya A, Zeniya M, Chikada H, Hyuck AD, Yamazaki Y, et al. SALL4, a stem cell biomarker in liver cancers. Hepatology 2013;57:1469–1483.
[36] Gonzalez-Roibon N, Katz B, Chaux A, Sharma R, Munari E, Faraj SF, et al. Immunohistochemical expression of SALL4 in hepatocellular carcinoma, a potential pitfall in the differential diagnosis of yolk sac tumors. Hum Pathol 2013;44:1293–1299.
[37] Yong KJ, Gao C, Lim JS, Yan B, Yang H, Dimitrov T, et al. Oncofetal gene SALL4 in aggressive hepatocellular carcinoma. N Engl J Med 2013;368: 2266–2276.
[38] Lai AY, Wade PA. Cancer biology and NuRD: a multifaceted chromatin remodelling complex. Nat Rev Cancer 2011;11:588–596.
[39] Marquardt JU, Thorgeirsson SS. Sall4 in "stemness"-driven hepatocarcinogenesis. N Engl J Med 2013;368:2316–2318.

European Journal of Immunology

Adipose tissue derived stromal stem cell therapy in murine ConA-derived hepatitis is dependent on myeloid-lineage and CD4$^+$ T-cell suppression

Mami Higashimoto[*1], *Yoshio Sakai*[*2,3], *Masayuki Takamura*[1], *Soichiro Usui*[1], *Alessandro Nasti*[1], *Keiko Yoshida*[1], *Akihiro Seki*[1], *Takuya Komura*[1], *Masao Honda*[3], *Takashi Wada*[2], *Kengo Furuichi*[4], *Takahiro Ochiya*[5] *and Shuichi Kaneko*[1,3]

[1] Disease Control and Homeostasis, Kanazawa University, Kanazawa, Japan
[2] Department of Laboratory Medicine, Kanazawa University, Kanazawa, Japan
[3] Department of Gastroenterology, Kanazawa University Hospital, Kanazawa, Japan
[4] Division of Blood Purification, Kanazawa University Hospital, Kanazawa, Japan
[5] Division of Molecular and Cellular Medicine, National Cancer Center Research Institute, Tokyo, Japan

Mesenchymal stromal stem cells (MSCs) are an attractive therapeutic model for regenerative medicine due to their pluripotency. MSCs are used as a treatment for several inflammatory diseases, including hepatitis. However, the detailed immunopathological impact of MSC treatment on liver disease, particularly for adipose tissue derived stromal stem cells (ADSCs), has not been described. Here, we investigated the immunomodulatory effect of ADSCs on hepatitis using an acute ConA C57BL/6 murine hepatitis model. i.v. administration of ADSCs simultaneously or 3 h post injection prevented and treated ConA-induced hepatitis. Immunohistochemical analysis revealed higher numbers of CD11b$^+$, Gr-1$^+$, and F4/80$^+$ cells in the liver of ConA-induced hepatitis mice was ameliorated after the administration of ADSCs. Hepatic expression of genes affected by ADSC administration indicated tissue regeneration-related biological processes, affecting myeloid-lineage immune-mediating Gr-1$^+$ and CD11b$^+$ cells. Pathway analysis of the genes expressed in ADSC-treated hepatic inflammatory cells revealed the possible involvement of T cells and macrophages. TNF-α and IFN-γ expression was downregulated in hepatic CD4$^+$ T cells isolated from hepatitis livers co-cultured with ADSCs. Thus, the immunosuppressive effect of ADSCs in a C57BL/6 murine ConA hepatitis model was dependent primarily on the suppression of myeloid-lineage cells and, in part, of CD4$^+$ T cells.

Keywords: Adipose tissue derived stromal stem cells · Anti-inflammatory effects · CD4$^+$ T cells · ConA hepatitis · Myeloid-lineage cells

Additional supporting information may be found in the online version of this article at the publisher's web-site

Correspondence: Dr. Shuichi Kaneko
e-mail: skaneko@m-kanazwa.jp

*These authors contributed equally to this work.

Introduction

Mesenchymal stromal stem cells (MSCs) are somatic cells that reside in the mesenchymal tissues, such as the BM, umbilical cord, and adipose tissue [1,2]. MSCs are able to differentiate into several types of cells (pluripotent) in the same lineage, such as chondrocytes, osteocytes, adipocytes, and cardiomyocytes, as well as those of different lineages, such as hepatocytes. Because of this differentiation capability, they have been studied as a possible application in regenerative therapy of miscellaneous impaired organs, such as breast reconstruction [3] and repair of ischemic heart tissue [4]. Another intriguing characteristic of MSCs is their immunomodulatory potency [5]. Because most liver diseases, including viral hepatitis [6,7], primary biliary cirrhosis [8], autoimmune hepatitis [9], and steatohepatitis [10], are associated with hepatic inflammatory cells [11], elucidation of the effect of MSCs on hepatic inflammation is important when considering the use of MSCs for treating liver diseases. Although the efficacy of MSC treatment of liver diseases has been reported [12], the detailed immunopathological impact of MSC treatment on liver diseases, particularly for adipose tissue derived stromal stem cells (ADSCs), has not been investigated.

ConA, a plant lectin [13], is frequently used to induce acute hepatitis in rodents [14] to model the pathological features of autoimmune hepatitis. Although this model is mediated mainly by lymphocyte-lineage cells such as T cells and NKT cells, Kupffer cells/macrophages also participate in hepatitis. Therefore, evaluating the therapeutic efficacy of ADSCs in this murine hepatitis model is important. Although the potential efficacy of ADSCs in a BALB/c ConA hepatitis model has been reported [15], the immunopathology has not been investigated.

We confirmed that immediate i.v. administration of ADSCs after ConA injection prevented hepatitis. We also observed that administering ADSCs 3 h after the ConA injection resulted in successful treatment of hepatitis, as the liver was already infiltrated by $CD11b^+$ and $Gr\text{-}1^+$ inflammatory cells. Gene expression analysis of the liver showed that ADSC treatment affected myeloid-lineage cells, providing repair and regenerative effects in ConA-induced hepatitis mice. Moreover, gene expression analysis of hepatic inflammatory cells indicated pathways related to T cells and monocyte-lineage cells. Pathologically important cytokines such as TNF-α and IFN-γ were upregulated in $CD4^+$ T cells isolated from ConA-induced hepatitis mice but were significantly suppressed by co-culture with ADSCs. Thus, the anti-inflammatory effects of ADSCs in the C57BL/6 murine ConA hepatitis model were mediated by the suppression of myeloid-lineage and $CD4^+$ T cells.

Results

Characteristics of the immune response in ConA-induced hepatitis mice

To examine the characteristics of ConA-induced acute hepatitis, we injected 300 μg ConA into C57BL/6 female mice ($n = 4$) and determined serum alanine transferase (ALT) and lactate dehydrogenase (LDH) activities. Serum ALT and LDH activities were elevated through 24 h (Fig. 1A). The macroscopic appearance and histology of the liver obtained 24 h after ConA injection revealed intense necrosis (Fig. 1B). The immunohistochemical analysis showed that the number of $CD4^+$ T cells in the liver peaked at 6 h after the ConA injection, and remained high for 24 h (Fig. 1C and D). The numbers of $CD11b^+$ cells and $Gr\text{-}1^+$ cells accumulated in the liver increased at 3 h and reached a maximum at 12 h after ConA injection (Fig. 1C and D). The numbers of $F4/80^+$ monocyte/macrophage lineage cells increased at 6 h after the ConA injection, but returned to basal levels after 24 h (Fig. 1C and D). We also assessed the frequency of $CD11b^+/Gr\text{-}1^+$ cells, as a phenotype of myeloid-derived suppressor cells (MDSCs), in ConA hepatitis mice at 6 h ($n = 3$). The frequency of $CD11b^+/Gr\text{-}1^+$ cells was higher than that in WT mice (Fig. 1E). Scavenger receptor CD204 expression was higher in $CD11b^+/Gr\text{-}1^+$ cells than $CD11b^+/Gr\text{-}1^-$ cells (Fig. 1F), and the population gated for $CD11b^+$ cells contained granulocytic $Ly\text{-}6C^+/Ly\text{-}6G^+$ cells as well as monocytic $Ly\text{-}6C^+/Ly\text{-}6G^-$ cells (Fig. 1G).

To determine the type of immune-mediating cells involved in ConA-induced acute hepatitis, we depleted mice of various immune cell subpopulations ($n = 4$ per group). Mice that were pretreated with clodronate, a reagent that depletes monocyte-macrophage lineage cells [16], followed by injection of ConA, did not show a significant elevation in serum ALT or LDH activity (Fig. 1H). Mild elevation of serum activity for these enzymes in mice depleted of $CD4^+$ T cells was observed, whereas depletion of $CD8^+$ T cells had no significant effect. These results suggest the importance of monocyte-macrophage myeloid-lineage cells, as well as the contribution of $CD4^+$ T cells, in ConA-induced hepatitis.

ConA-induced acute hepatitis is ameliorated by i.v. administration of ADSCs in vivo

Next, we determined the therapeutic efficacy of ADSCs in the ConA-induced hepatitis model. We obtained and expanded stromal cells from adipose tissue by passaging them eight to ten times (Fig. 2A). Almost all cells expressed the mesenchymal lineage markers, CD29 and CD44 (Fig. 2B). With regard to stem cell markers [17], approximately 40% and 73% of cells expressed CD105 and CD90, respectively (Fig. 2B). Moreover, the cells were pluripotent and were able to differentiate into osteocytes, chondrocytes, and adipocytes (Fig. 2C–F). When 1×10^5 ADSCs were administered via the tail vein immediately after ConA injection in mice ($n = 3$), the elevation of serum ALT and LDH activity was substantially ameliorated, compared with mice without ADSC treatment ($n = 4$) 24 h after injection (Fig. 3A). In terms of therapeutic efficacy, 1×10^5 ADSCs were administered to mice 3 h after ConA injection ($n = 3$), serum ALT and LDH activities were significantly reduced in acute hepatitis mice treated with ADSCs, compared with ConA-induced hepatitis mice without treatment ($n = 4$), 24 h after ConA administration (Fig. 3B). The macroscopic

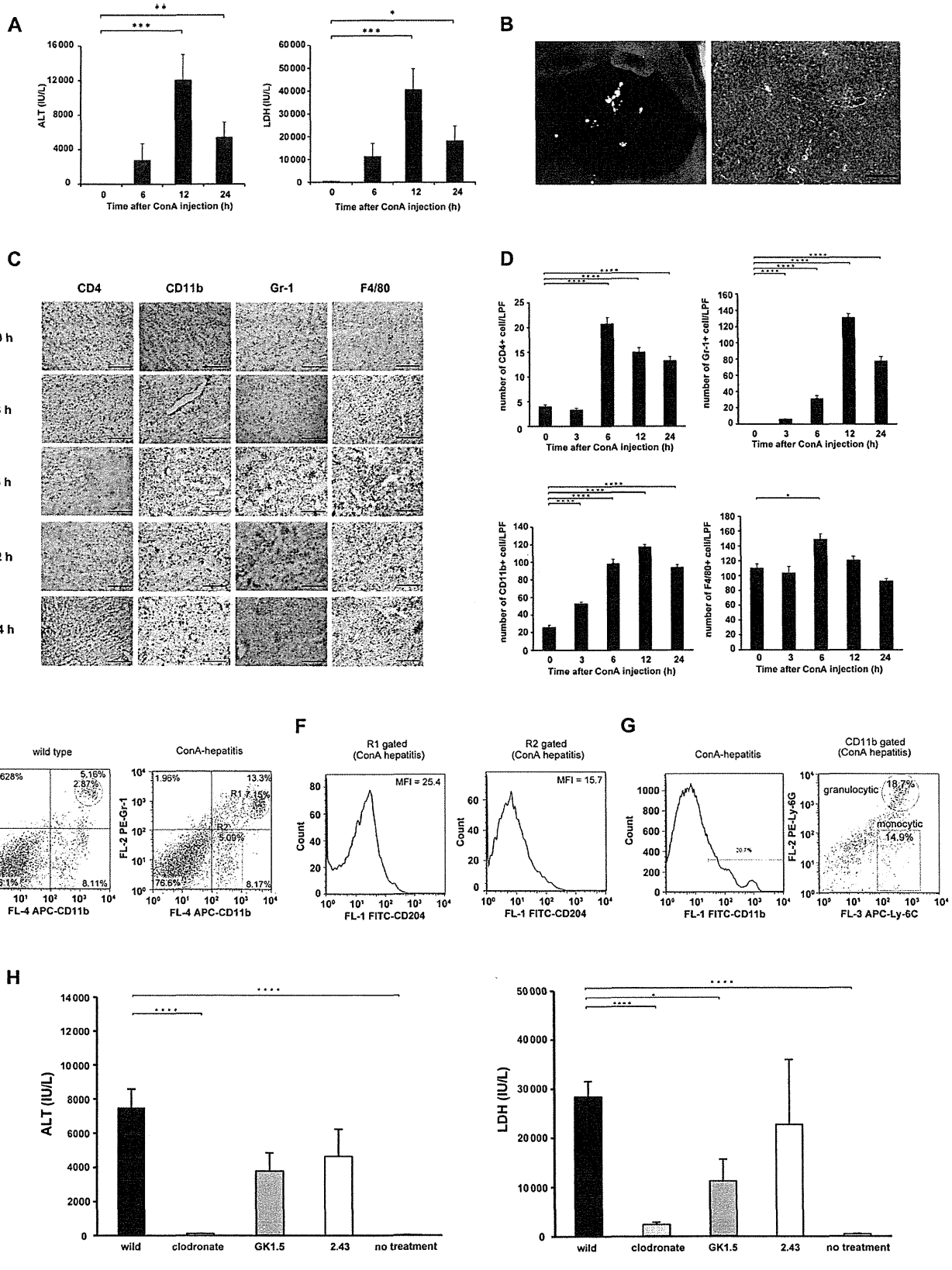

appearance of the liver obtained from mice injected with 300 μg of ConA followed by ADSC administration showed a mild and spotty white area with an almost normal color (Fig. 3C). Liver histology showed an almost normal appearance, with no necrosis (Fig. 3C), indicating that ConA-induced hepatitis was markedly ameliorated by ADSC treatment. No preventive or therapeutic effect on ConA-induced hepatitis resulted from administration of primary cultured murine hepatocytes ($n = 3$); there was no significant reduction in serum ALT or LDH (Fig. 3A and B), macroscopic necrosis appearance, or histological necrosis, compared with ConA-induced hepatitis (Fig. 3C).

ADSC treatment reduces elevated cytokine/chemokine concentrations in ConA-induced hepatitis mice

Marked protective and therapeutic effects of ADSCs on ConA-induced hepatitis were observed. To determine the effect of ADSC treatment on systemic inflammation in ConA-induced hepatitis, we measured serum cytokine and chemokine concentrations in ConA-induced hepatitis mice treated with ADSCs. Mice injected with ConA were immediately treated with ADSCs and serum was collected 6 h after ConA injection ($n = 3$). The elevated serum IFN-γ, IL-2, IL-6, IL-4, IP-10, MIG, KC, and MCP-1 levels in ConA-injected mice ($n = 3$) were significantly reduced by ADSC treatment (Supporting Information Fig. 1A). Injection of mice with ADSCs 3 h after ConA administration ($n = 4$) resulted in significantly reduced serum IFN-γ, IL-2, IL-6, and MIG levels, compared to ConA-injected mice not treated with ADSCs ($n = 6$) (Supporting Information Fig. 1B). Thus, the levels of the array of cytokines and chemokines that are elevated in the sera of ConA-induced hepatitis mice were significantly decreased by ADSC treatment.

Distribution of i.v. administered ADSCs in ConA-induced hepatitis murine models

The distribution of administered ADSCs in ConA-induced hepatitis mice was determined by immunohistochemistry. Administered GFP-expressing ADSCs were observed in the lung, but not the liver, of mice injected with ConA followed by immediate ADSC administration ($n = 6$), through 24 h (Supporting Information Fig. 2A). When administered to mice 3 h after ConA injection ($n = 6$), GFP-expressing ADSCs were observed primarily in the lung, and a few in the liver (Supporting Information Fig. 2B), suggesting that some fraction of ADSCs reached the liver upon occurrence of hepatitis.

Hepatic gene expression changes by ADSCs treatment are associated with Gr-1$^+$ and CD11b$^+$ cells

To investigate the detailed biological features of the liver in ConA-induced hepatitis mice that were treated with ADSCs, we examined the gene expression profiles of liver tissue of ConA-injected mice obtained 2 h after treatment with ADSCs using a DNA microarray. In the liver tissues of mice treated with ADSCs immediately after ConA injection ($n = 3$), 589 gene probes were differentially expressed compared with that in mice with ConA-induced hepatitis that had not been treated with ADSCs ($n = 3$). Expression of the majority of genes was downregulated by ADSCs, as shown by green color ($p < 0.05$; Fig. 4A). Principal component analysis using these genes showed a discernible distribution difference between the ADSC-treated and -untreated groups (Fig. 4B). When mice received ADSC treatment 3 h after ConA injection, hepatic expression of 309 gene probes was altered significantly compared with those in mice with ConA-induced hepatitis that had not been treated with ADSCs ($n = 3$). Expression of the majority of genes was downregulated by ADSCs, as shown by green color ($p < 0.01$; Fig. 4C). Principal component analysis of these genes also showed a discernible distribution difference between the ADSC-treated and untreated groups (Fig. 4D). In the context of biological maps of the genes affected by immediate ADSC treatment, cell differentiation, the inflammatory response, the DNA damage response, and apoptosis predominated (Supporting Information Table 1). In addition to these maps, tissue remodeling and wound repair, mitogenic signaling, and vascular development (angiogenesis) predominated in mice that had received ADSC treatment 3 h after ConA injection (Table 1), indicating that ADSCs provided not only anti-inflammatory effects, but also remodeling effects, in the ConA-damaged liver.

◀ **Figure 1.** Characteristics of ConA-induced hepatitis in C57BL/6 mice. (A–D) C57BL/6 female mice were injected i.v. with 300 μg of ConA. Sera and liver tissues were obtained 3, 6, 12, and 24 h after ConA injection. The data are representative of three individual experiments. (A) ALT and LDH activity in sera. Results are expressed as means ± SE ($n = 4$). $^*p < 0.05$, $^{**}p < 0.01$, $^{***}p < 0.005$ versus 0 h (Student's t-test). (B) Representative liver tissues obtained 12 h after ConA injection were assessed macroscopically and microscopically. Magnification: ×100. Bar: 200 μm. (C) Immunohistochemical staining for CD4, CD11b, Gr-1, and F4/80 in the livers of mice for each time point (0, 3, 6, 12, and 24 h; $n = 4$ per time point). Representative images of mice for each time point are shown. Magnification: ×100. Bar: 200 μm. (D) Quantification of the number of CD4$^+$, CD11b$^+$, Gr-1$^+$, and F4/80$^+$ cells in four visual fields per ×100 low-power field in the livers of representative mice in each group. Magnification: ×100. $^*p < 0.05$, $^{****}p < 0.001$ versus untreated mice (Student's t-test). (E–G) Hepatic inflammatory cells were isolated from mice 6 h after ConA injection, incubated with fluorescence-conjugated antibodies, and assessed by FACS. Three mice per group per experiment. Experiments were performed twice. (E) Frequency of CD11b$^+$Gr-1$^+$ cells in WT C57BL/6 mice and ConA hepatitis mice. (F) Analysis of CD204 expression in CD11b$^+$Gr-1$^+$ cells (R1-gated region in (E)) and CD11b$^+$Gr-1$^-$ cells (R2-gated region in (E)) among hepatic inflammatory cells from ConA hepatitis mice. MFI: mean fluorescence intensity. (G) CD11b$^+$ cells among hepatic inflammatory cells from ConA hepatitis mouse were gated, and Ly-6C and Ly-6G expression levels in the gated cells were determined. (H) C57BL/6 female mice were injected i.v. with clodronate ($n = 4$), i.p. with anti-CD4 antibody (GK1.5) ($n = 4$), or anti-CD8 antibody (2.43) ($n = 4$) every 24 h for 2 days. The mice were then injected i.v. with 300 μg of ConA. Sera were obtained 24 h after ConA injection, and ALT and LDH activities were then measured. Results are expressed as means +SE ($n = 4$ per group) and are representative of one experiment performed. $^*p < 0.05$, $^{****}p < 0.001$ versus ConA-injected WT mice ($n = 4$) (Student's t-test).

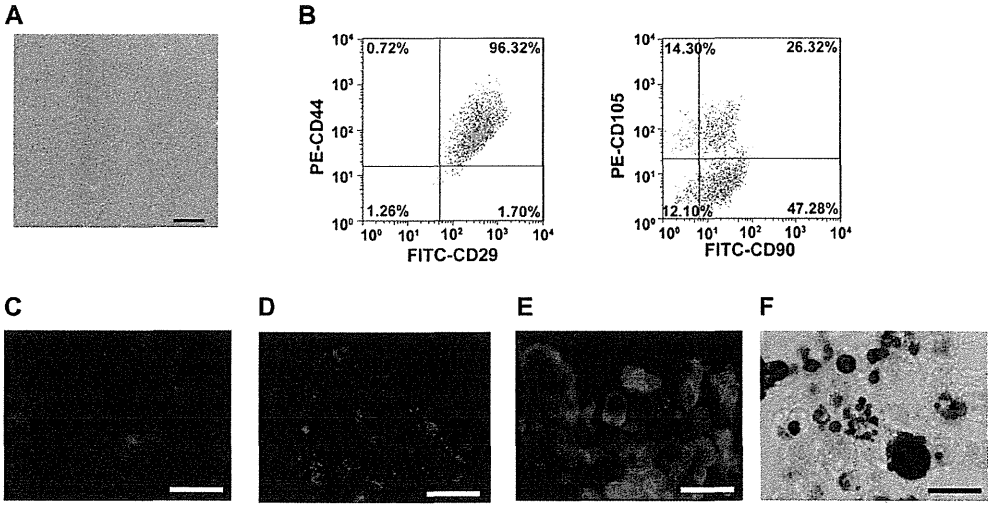

Figure 2. Characteristics and pluripotency of cultured ADSCs. Cells in the stromal fraction of adipose tissues from mice were cultured, maintained, and expanded for eight to ten passages. (A) Spindle shaped cells were observed after eight passages. Magnification: ×100. Bar: 200 μm. (B) Flow cytometric analysis of CD29, CD44, CD90, and CD105 surface marker expression. The data shown are representative of three independent experiments. (C–F) ADSCs were cultured with specific growth factors for induction of osteocytes, chondrocytes, and adipocytes using a mouse mesenchymal stem cell functional kit. Immunohistochemical staining was performed with (C) anti-osteopontin antibody for osteocytes, (D) anti-collagen II antibody for chondrocytes, and (E) anti-FABP antibody as well as (F) Oil-Red O staining for adipocytes. Magnification: x200. Bars: 50 μm. All data shown are from one experiment representative of two independent experiments performed.

Next, we investigated the relevance of these altered genes in the context of inflammatory cells using the public gene expression database of hematopoietic cells and stem cells (GSE27787). The annotated genes among the 589 gene probes detected by microarray analysis probes in the livers of mice that received ADSC treatment immediately after ConA injection were not relevant to any hematopoietic cell type (Fig. 4E). By contrast, among the 309 gene probes, the majority of the annotated genes whose hepatic expression in mice that received ADSC treatment 3 h after ConA injection was affected significantly were found to be highly expressed in Gr-1$^+$ cells and Mac1$^+$ (CD11b$^+$) cells — as indicated by the red color (Fig. 4F). Since majority of the 309 gene probes in the liver of ConA hepatitis were downregulated by ADSC treatment, as indicated by green color (Fig. 4C), these results suggested that effects on Gr-1$^+$ and CD11b$^+$ cells were associated with the therapeutic effect of ADSCs 3 h after ConA injection.

ADSC treatment represses inflammatory cell accumulation in ConA-induced hepatitis

To determine the influence of ADSC treatment on the infiltration/accumulation of immune-mediating cells in the liver of ConA-induced hepatitis mice, we assessed by immunohistochemistry the inflammatory cells in the liver tissues of mice injected with ConA followed by ADSC administration at 3 h. Liver tissues obtained at 6, 12, and 24 h (n = 4 each time point) after ConA injection showed reduced accumulation of CD11b$^+$ cells, Gr-1$^+$ cells, and F4/80$^+$ cells after ADSC treatment (Fig. 5). In contrast, the increased number of infiltrated CD4$^+$ T cells in ConA-induced hepatitis mice was not significantly affected by the ADSCs (Fig. 5). Thus, the predominant change in ConA-induced hepatitis mice treated with ADSCs was in the number of myeloid-lineage inflammatory cells, consistent with the hepatic gene expression data.

T-cell involvement in the altered gene expression of hepatic inflammatory cells by ADSCs treatment

To further assess the anti-inflammatory effects of ADSCs in mice with ConA-induced hepatitis, we isolated hepatic inflammatory cells from mice 2 h after ADSC treatment, which was administered 3 h after ConA injection (n = 2) and from mice not treated with ADSCs (n = 2). A total of 939 genes were differentially expressed in hepatic inflammatory cells from ConA-induced hepatitis mice treated with ADSCs. The gene expression profiles associated with ADSC treatment and ConA-induced hepatitis without ADSC treatment were readily distinguishable (Supporting Information Fig. 3A). Pathway map analysis showed that these genes were relevant to biological pathways of oncostatin M signaling via JAK-Stat or MAPK signaling and CCR5 signaling in macrophages and T lymphocytes in the immune response pathway (Supporting Information Table 2). Network analysis of these genes featured a network consisting of AcRIIA, STAT3, Activin A, FTSJD1, and STAT1 at the top (Supporting Information Table 3), which indicated that pathways involving IL-2 and TNF-α, and the STAT1/STAT3 pathway were also involved (Supporting Information Fig. 3B). These results suggest that T cells, as well as antigen presenting/phagocytosis lineages, were the immune-mediating cell populations affected by ADSC treatment.

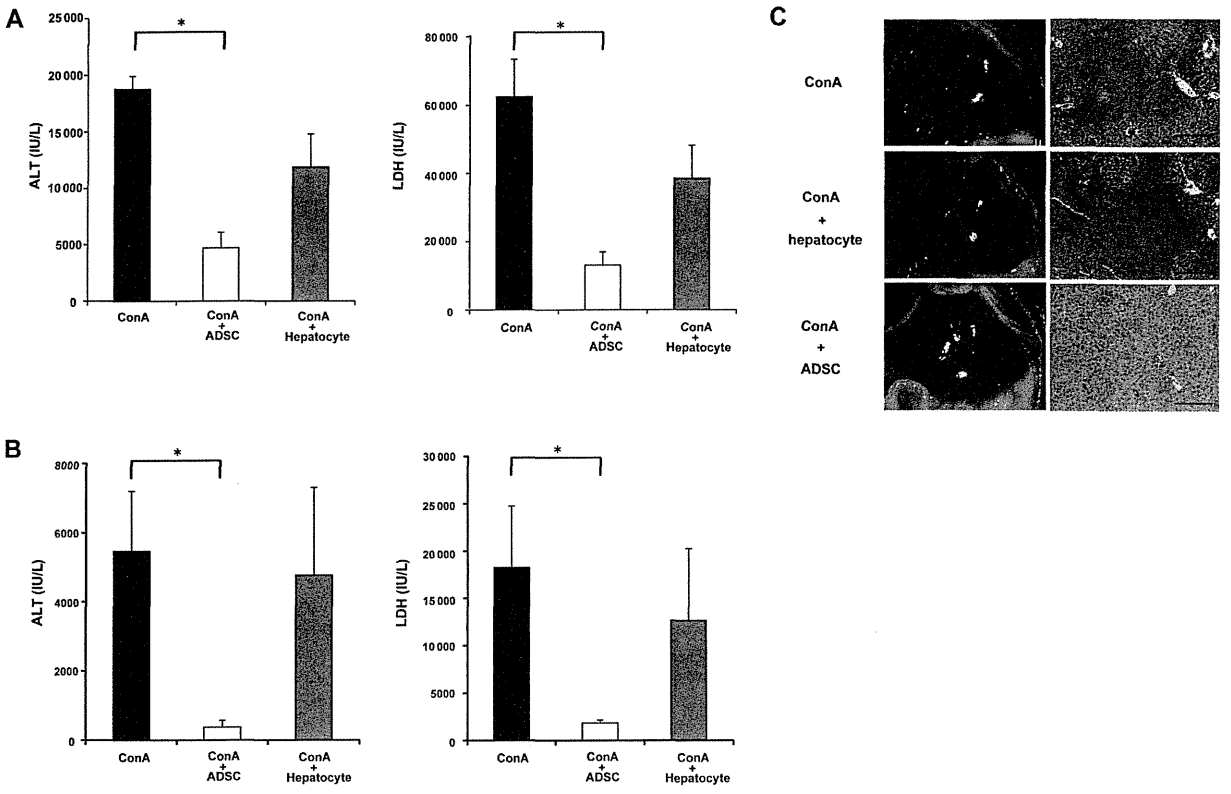

Figure 3. Therapeutic effects of ADSCs in ConA-induced hepatitis. C57BL/6 female mice were injected i.v. with 300 μg of ConA. Immediately or 3 h later, 1×10^5 ADSCs or hepatocytes were injected via the tail vein. Liver tissues and blood samples were obtained 24 h after ConA injection. Liver tissues were examined histologically and serum ALT and LDH activities were measured. (A, B) Serum ALT and LDH activities of mice injected with ConA followed by ADSC injection (A) immediately or (B) 3 h later. ConA: ConA-injected mice without treatment ($n = 4$), ConA + ADSC: ConA-injected mice followed by ADSC treatment ($n = 3$), ConA + hepatocyte: ConA-injected mice followed by primary cultured hepatocyte treatment ($n = 3$). Data are shown as mean ± SE and are from one experiment representative of two independent experiments. $^*p < 0.05$ (Wilcoxon signed-rank test), compared with ConA-injected mice. (C) Macroscopic appearance of the liver (left) and histology of the liver tissues as assessed by H&E staining (right). Magnification of histology: ×100. Bars: 200 μm. Images shown are from one mouse representative of three to four mice from each group studied.

ConA-activated CD4$^+$T cells and CD11b$^+$ cells in the liver are important targets of ADSC treatment

The above data indicated that ADSCs administered in ConA-induced hepatitis had therapeutic immunological effects in terms of repairing the damaged liver and affected CD11b$^+$ and Gr-1$^+$ myeloid-lineage cells and T cells. To further explore how ADSCs affected the subpopulations of inflammatory cells involved in ConA-induced hepatitis, we investigated the expression of cytokine/chemokine-related genes in CD4$^+$ T cells and CD11b$^+$ cells obtained from livers with ConA-induced hepatitis ($n = 4$) that had been treated in vitro with ADSCs ($n = 3$). Expression of TNF-α, IL-10, and CXCL10 was significantly downregulated by ADSC treatment in both CD4$^+$ T cells (Supporting Information Fig. 4A) and CD11b$^+$ cells (Supporting Information Fig. 4B). IFN-γ, IL-4, and CXCL9 expression by CD4$^+$ T cells were significantly affected by ADSCs. Although CCL3, which was upregulated by ConA injection, was not significantly affected by ADSCs, the expression of its cognate receptor, CCR5, was decreased in CD4$^+$ T cells (Supporting Information Fig. 4A), suggesting an effect on the CCL3-CCR5 axis. These results suggest that CD4$^+$ T cells and myeloid-lineage CD11b$^+$ cells were the susceptible hepatic inflammatory subpopulations of cells in the ConA-induced hepatitis liver.

Anti-inflammatory effect of ADSCs on ConA hepatitis do not rely on MDSCs

We further assessed whether the anti-inflammatory effect of ADSCs in ConA hepatitis relied on MDSCs. Neither the frequency of nor the NO production by CD11b$^+$Gr-1$^+$ cells were increased by ADSC treatment (Supporting Information Fig. 5A). CD11b$^+$Gr-1$^+$ cells from ConA-injected mice treated with ADSCs showed arginase activity similar to that in CD11b$^+$Gr-1$^+$ cells from ConA-injected mice (Supporting Information Fig. 5B). CD11b$^+$Gr-1$^+$ cells from ConA-injected mice treated with ADSCs suppressed the ConA-stimulated proliferation of T cells in vitro, although the effect was slightly attenuated compared to that of cells from mice with ConA-induced hepatitis (Supporting Information Fig. 5C). Thus, ADSC treatment was not dependent on MDSCs induced by ConA hepatitis.

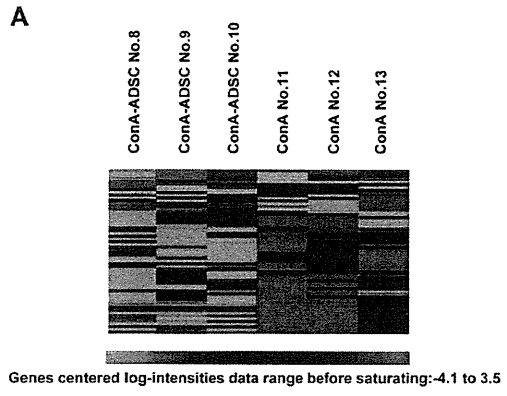

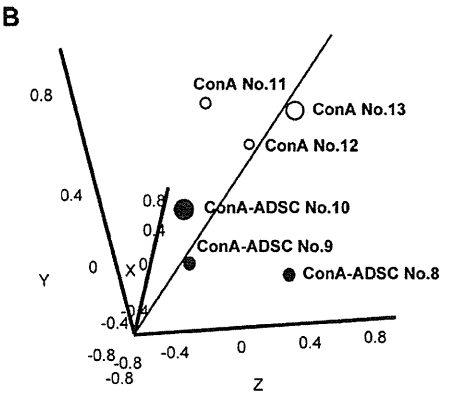

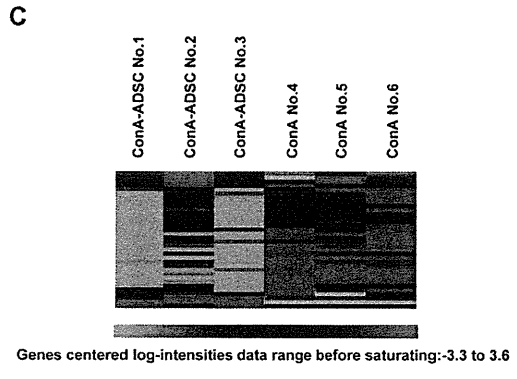

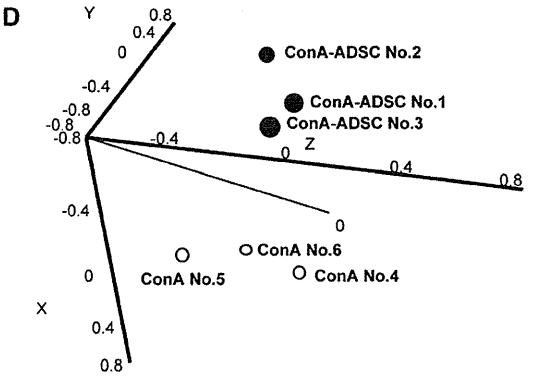

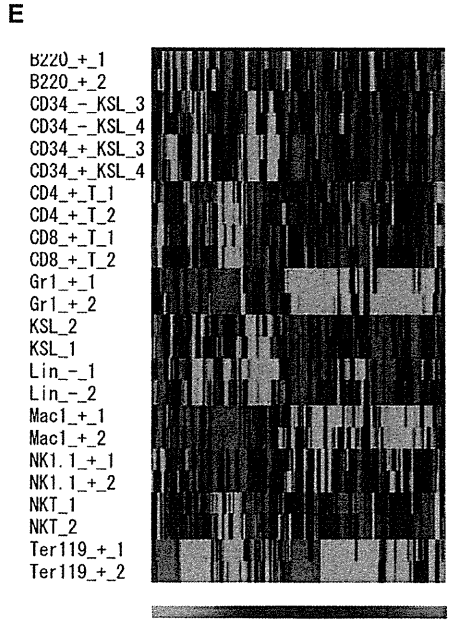

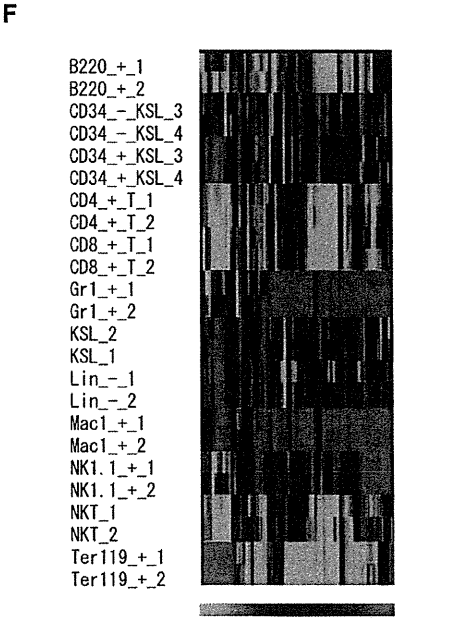

Discussion

MSCs are effective for immune-mediated disease treatment including the ConA-induced BALB/c murine hepatitis model [15], but the detailed mechanisms have not been fully elucidated. Here, we confirmed that ADSCs have preventive and therapeutic effects in a ConA-induced C57BL/6 hepatitis murine model and assessed the immunopathological mechanisms by determining the participating hepatic immunomodulatory cells. ADSCs injected via the tail vein were found in the lung; some were observed in the liver but only when ADSCs were administered 3 h after ConA injection, a time at which infiltration of $CD11b^+$ and $Gr\text{-}1^+$ inflammatory cells into the liver had already begun. Gene expression analysis of liver tissue from ConA-induced hepatitis mice showed that the ADSC treatment induced biological pathways indicative of liver repair and regeneration. Myeloid-lineage cells were the predominant population in terms of affected genes, consistent with immunohistochemical staining of the liver for immune-mediating cells. Furthermore, the gene expression profiles of hepatic inflammatory cells from ConA-induced hepatitis mice treated with ADSCs suggested T-cell and macrophage involvement. Moreover, the expression patterns of cytokine/chemokine-related genes in hepatic inflammatory cells co-cultured with ADSCs suggested that $CD4^+$ T cells were important in ConA-induced hepatitis and were affected by ADSC treatment.

The immunopathological features of ConA-induced hepatitis have been characterized as being primarily lymphocyte-lineage cell-mediated hepatitis [18–20], leading to massive hepatocellular degeneration, necrosis, and apoptosis [21]; thus, this model is relevant to clinical autoimmune hepatitis. Additionally, Kupffer cells play an important role in induction of hepatitis [22]. Unexpectedly, we observed prominent increases in $CD11b^+$, $Gr\text{-}1^+$, and $F4/80^+$ cells in liver tissues of the ConA-induced hepatitis mice. Additionally, we found that the monocyte-macrophage lineage cells contributed most significantly to hepatitis, as confirmed by depletion treatment, such that hepatitis was almost completely abolished when those cell types were abrogated by clodronate. This is further evidenced by the fact that ADSC treatment reduced the number of $CD11b^+$, $Gr\text{-}1^+$, and $F4/80^+$ cells in the liver of ConA-induced hepatitis mice (Fig. 5). The importance of $Gr\text{-}1^+$ and $CD11b^+$ cells was also suggested by changes in the gene expression profile of the liver of ConA-induced hepatitis treated with ADSCs (Fig. 4C and F). Thus, monocyte-macrophage lineage cells are important in the pathogenesis of ConA-induced hepatitis in mice and are important targets of ADSCs. $CD4^+$ T cells were also involved since their depletion partially ameliorated ConA-induced hepatitis. The number of infiltrating $CD4^+$ T cells in the liver of ConA-induced hepatitis mice was not markedly reduced by ADSC treatment. However, gene expression analysis of hepatic inflammatory cells in ConA-induced hepatitis mice treated with ADSCs showed that signaling of oncostatin M, a type I cytokine associated with developing T cells [23], and CCR5 signaling in macrophages and T lymphocytes were affected. Therefore, $CD4^+$ T cells participate as an immune mediator and therapeutic target of ADSCs in the pathology of ConA-induced hepatitis mice.

With regard to cytokine/chemokine-related gene expression in hepatic inflammatory cells of ConA-induced hepatitis mice, expression of TNF-α, IL-10, and CXCL10 in $CD4^+$ T cells and $CD11b^+$ cells was downregulated by ADSC treatment (Supporting Information Fig. 4). Additionally, IFN-γ, IL-4, and *CXCL9* were also significantly downregulated in $CD4^+$ T cells, but not in $CD11b^+$ cells (Supporting Information Fig. 4). Changes in the expression of the Th2 cytokines, IL-10 and IL-4, were considered to be the secondary consequence of ConA-induced hepatitis, mediated by TNF-α and/or IFN-γ, which are characterized as Th1-associated cytokines [24]. CCR5 expression by $CD4^+$ T cells was downregulated by ADSCs, which may be relevant to the biological processes indicated by the downregulated genes in hepatic inflammatory cells. Because CCR5 is a $CD4^+$ T-cell receptor that interacts with APCs, such as macrophages [25], suppression of CCR5 expression on $CD4^+$ T cells by ADSC might explain the amelioration of ConA-mediated hepatitis. Overall, the therapeutic efficacy of ADSCs impacted both $CD4^+$ and $CD11b^+$ cells in terms of alteration of levels of inflammatory humoral mediators and cytokine/chemokine profiles, thus contributing to amelioration of ConA-induced hepatitis.

A proportion of i.v. administered ADSCs were present in the livers of ConA mice injected with ADSCs at a time point at which the liver had already been infiltrated with $Gr\text{-}1^+$ and $CD11b^+$ cells, whereas no ADSCs were present in the livers of mice injected with ConA following immediate treatment with ADSCs. This indicates that a liver undergoing inflammation attracts administered ADSCs. The extent of inflammation required to recruit ADSCs should be clarified, as it has previously been reported that hepatitis occurring just 30 min after ConA injection results in recruitment of a substantial number of stem cells to the liver in the BALB/c ConA hepatitis model [15]. Given that the migratory capabilities of MSCs are well known although not yet fully investigated [26], how ADSCs are recruited to an already inflamed liver as a result of ConA administration should be examined. In addition, the ADSCs administered to C57BL/6 mice immediately after ConA injection resided in the lung. In spite of the fact that they were not detected in the liver, these ADSCs prevented ConA hepatitis, indicating the remote effect of ADSCs. Thus, indirect mediators produced by ADSCs associated with their anti-inflammatory effects should be investigated intensively.

◀ **Figure 4.** Gene expression analysis in the liver of ConA-induced hepatitis mice treated with ADSCs. C57BL/6 female mice were injected i.v. with 300 μg of ConA. (A, B, and E) Immediately or (C, D, and F) 3 h after ConA injection, mice were treated with 1×10^5 ADSCs via the tail vein ($n = 3$ each). Liver tissues were analyzed 2 h after ADSC administration and RNA was isolated for gene expression analysis using a DNA microarray. Data shown are from one experiment performed. (A, B) One-way clustering analysis (A) and principal component analysis (B) of the 589 differentially expressed genes in treated and untreated ConA-injected mice. (C, D) One-way clustering analysis (C) and principal component analysis (D) of the 309 differentially expressed genes in treated (after 3 h) and untreated ConA-injected mice followed. Colors indicate the intensity of gene upregulation (red), downregulation (green), and no change (black). (E, F) One-way clustering analysis of gene expression in hematopoietic and stem cells (GSE27787) for annotated genes among the 589 (E) and 309 (F) genes.

Table 1. Maps relevant to genes for which the expression was affected in the liver of ConA-injected mice followed by ADSC treatment at 3 h.

Maps	*p*-value
Tissue remodeling and wound repair	0.000001438
Inflammatory response	0.000003973
Mitogenic signaling	0.0001056
Vascular development (angiogenesis)	0.0002926
DNA damage response	0.0004529
Apoptosis	0.0008909
Cystic fibrosis disease	0.001402
Myogenesis regulation	0.001571
Cell differentiation	0.002173
Immune system response	0.003304

In conclusion, the therapeutic anti-inflammatory efficacy of ADSCs relied on suppression of myeloid-lineage and $CD4^+$ T cells in the ConA-induced C57BL/6 murine hepatitis model. The application of ADSC therapy to various inflammatory liver diseases can be further developed by studies of their immunomodulatory effects.

Materials and methods

Murine acute hepatitis induced by ConA injection and treatment with ADSCs

C57BL/6J female mice (10–12 weeks old, Charles River Laboratories Japan Inc., Yokohama, Japan) were injected i.v. with 300 μg of ConA (Sigma-Aldrich, St. Louis, MO, USA) dissolved in PBS. For $CD4^+$ T-cell or $CD8^+$ T-cell depletion, 200 μg of purified anti-CD4 antibody from the culture supernatant of GK1.5 cells (ATCC, Manassas, VA, USA), or purified anti-CD8 antibody from the culture supernatant of 2.43 cells (ATCC), was injected i.p. for two consecutive days before ConA injection. For depletion of monocyte-macrophage lineage cells, 2 mg of clodronate (Sigma-Aldrich), which was encapsulated in liposomes using the COATSOME-EL-01-N liposome formulation kit (Nihonyushi, Tokyo, Japan) [27], was injected via the tail vein 2 days before ConA injection. For the prevention or treatment experiment, 1×10^5 ADSCs were administered i.v. immediately or 3 h after ConA injection. In some cohorts, blood was obtained under anesthesia, and liver and lung tissues were collected after euthanizing mice at 6, 12, and 24 h after ConA injection. A portion of the liver tissue was homogenized and the enriched fraction of inflammatory cells was obtained by gradient centrifugation using Ficoll–Hypaque (Sigma-Aldrich). Our institutional review board approved the care and use of laboratory animals in all experiments.

Isolation and culture of ADSCs and primary hepatocytes

Inguinal adipose tissues were obtained from C57BL/6J male mice (10–12 weeks old, Charles River Laboratories Japan Inc.) or GFP-transgenic mice (male, 10–12 weeks old, gift from Prof. Okabe, Osaka University, Japan). Tissues were digested with 0.075% collagenase type I (Wako Pure Chemical Industries Ltd., Osaka, Japan), washed with PBS, and then transferred to a culture dish with DMEM/F-12 1:1 medium (Life Technologies–Invitrogen, Carlsbad, CA, USA) supplemented with 10% heat-inactivated FBS and 1% antibiotic–antimycotic solution (Life Technologies). Cells were maintained and expanded by eight to ten passages before use.

To obtain primary hepatocytes, C57BL/6J male mice (10–12 weeks old) were anesthetized by i.p. injection of pentobarbital (50 mg/kg; Kyoritsu Seiyaku, Tokyo, Japan) and injected with 10 mL of 0.75% type I collagenase solution via the portal vein. Liver tissues were minced to dissociate cells, filtered through a 100 μm mesh, and cultured in 10-cm culture dishes for 16 h until use.

Pluripotency of ADSCs

The pluripotency of ADSCs was examined using a mouse mesenchymal stem cell functional kit® (R&D Systems, Minneapolis, MN, USA), and immunohistochemical staining of cells that had differentiated into osteocytes, chondrocytes, and adipocytes was performed using anti-mouse ostepontin, anti-mouse collagen II, and anti-mouse FABP4 antibodies, respectively, in accordance with the manufacturer's instruction. Adipocyte differentiation was also assessed by staining using an aliquot of Oil Red O (WAKO).

Co-culture of ConA-stimulated hepatic inflammatory cells with ADSCs

Hepatic inflammatory cells were isolated from C57BL/6J female mice (10 weeks old) that had been injected i.v. with 300 μg of ConA 3 h before ($n = 4$). $CD4^+$ T cells and $CD11b^+$ cells were separated from the collected hepatic inflammatory cells using anti-CD4 and anti-CD11b magnetic beads (Miltenyi Biotec, Bergisch Gladbach, Germany). Then, 20 000 ADSCs were co-cultured with 4×10^5 of the isolated $CD4^+$ T cells or $CD11b^+$ cells in a 24-well plate (BD Falcon, San Jose, CA, USA) for 2 h ($n = 3$). After co-culture, floating cells were harvested, and RNA harvested using the MicroRNA isolation kit (Stratagene, La Jolla, CA, USA) for real-time PCR analysis to measure cytokine/chemokine gene expression.

Measurement of serum ALT and LDH activity

Blood was collected from the postorbital venous plexus and serum was separated from clotted blood after coagulation. The serum activity of ALT, and LDH was measured using L-type WAKO GPT J2, and LDH-J kits (Wako Pure Chemical Industries Ltd.), respectively, using autoanalytical equipment (Hitach7180, Hitachi Ltd., Tokyo, Japan), according to the manufacturer's protocol.